C. 2

NACA

RESEARCH MEMORANDUM

TEMPERATURE-CONTROL STUDY OF TURBINE REGION OF TURBOJET ENGINE, INCLUDING TURBINE-BLADE TIME CONSTANTS AND STARTING CHARACTERISTICS

By W. E. Phillips, Jr.

Lewis Flight Propulsion Laboratory
Cleveland, Ohio

NATIONAL ADVISORY COMMITTEE
FOR AERONAUTICS

WASHINGTON
April 25, 1956

NACA RM E55L22

NATIONAL ADVISORY COMMITTEE FOR AERONAUTICS

RESEARCH MEMORANDUM

TEMPERATURE-CONTROL STUDY OF TURBINE REGION OF TURBOJET ENGINE, INCLUDING TURBINE-BLADE TIME CONSTANTS AND STARTING CHARACTERISTICS

By W. E. Phillips, Jr.

SUMMARY

An investigation was made of a turbojet engine in an altitude test facility to supplement existing data relevant to gas-temperature control in a turbojet engine. The problems associated with gas-temperature control for minimizing turbine-blade damage are considered in this report.

Steady-state temperature distributions, including the turbine-blade temperatures, were investigated at rated engine speed for a range of altitudes and flight speeds. The tail-pipe gas temperature was found to be most indicative of the turbine-blade temperature over a range of operation. For all conditions considered, the tail-pipe gas temperature was between 180° and 210° F lower than the maximum turbine-blade temperature.

The dynamic responses of the turbine-blade temperatures to the tail-pipe gas temperature at actual rated engine speed were evaluated over a range of altitudes. For all conditions, the dynamic responses were found to be essentially first-order lags. For this reason, the blade-temperature dynamic response may be represented by a characteristic time constant. These blade time constants vary with position on the blade, the leading edge having the shortest time constant, the trailing edge slightly longer, and the midchord time constant longer than the leading-edge time constant by a factor of two.

The time constants for the trailing edge and midchord portions of the turbine blade were calculated and showed good agreement with the experimental results.

The time constants increased with an increase in altitude, and this variation correlated very well with a theoretical calculated variation. The calculated variation indicated that the blade time constants varied inversely as 0.8 power of engine air flow.

Data were taken in the region from start to idle in order to determine the acceleration characteristics of the engine as a function of tail-pipe gas temperature. At each engine speed during the transient from start to idle, a definite maximum acceleration obtainable was found. Over the majority of the speed range from start to idle, this maximum occurred at a tail-pipe gas temperature of less than 1400° F.

INTRODUCTION

The object of this report is to discuss and supplement existing data relevant to the problem of gas-temperature control within a turbojet engine. Two operating regions of the engine where blade failures are most prevalent are considered. These regions are the rated-power regions where stress-rupture failures are prevalent, and the starting regions where thermal-stress failures may occur because of adverse temperature patterns through the blades.

In the rated-power region of operation, current practice is to use the tail-pipe gas temperature as the gas-temperature control signal. Limits determined from engine-damage records for the particular engine are imposed on the gas temperature to prevent damage to the turbine blades. The difference between tail-pipe gas temperature and turbine-blade temperature varies, however, with operating conditions, and this deviation may impose unnecessary restraints on the engine thrust in the interests of turbine-blade safety. As an indication of the relative sensitivity of thrust and blade life at rated engine power for a current engine, if the turbine-inlet gas temperature is increased to give a 10-percent increase in thrust, the stress-rupture life of the blade is decreased by 90 percent.

In order to realize more of the capabilities of the engine in the rated-power region without appreciably reducing the engine life, a temperature-control signal more accurate than the tail-pipe gas temperature may be required. Steady-state temperature data in the region of the turbine, including the turbine-blade temperatures, are presented in references 1 and 2. These references, however, do not discuss the problem from the control viewpoint.

The seriousness of the temperature problem in the rated-power region is tempered somewhat when the turbine-blade dynamics are considered. The mass of the turbine blade prevents the turbine-blade temperature from immediately following a change in the surrounding gas temperature. Analytical and experimental results in reference 3 show that the response of blade temperature to a step in gas temperature approximates very closely a first-order lag, and the dynamics of the turbine-blade temperature may be characterized by time constants. These blade dynamics allow short bursts of overrated power without overtemperaturing the

turbine. References 3 and 4 contain the only previous experimental study of turbine-blade temperature dynamics, but the study was limited to sea-level data. Before the restrictions on engine gas temperature during transient operation can be safely relaxed, the variation of the blade time constant must be determined over a range of altitudes at rated engine rotor speed.

The blade-failure problem in the starting cycle of a turbojet engine results from the rapid changes in gas temperature as the engine is started and accelerated to the idle engine speed. These rapid changes may cause turbine-blade damage because of adverse temperature patterns. The trend has been to assume that a higher gas temperature will result in better acceleration characteristics from start-to-idle engine speed. This method unfortunately increases the tendency of damage to the turbine blades. It is desirable then to investigate the engine behavior in the transient condition from engine start to engine idle.

The scope of this report covers three phases of the temperature-control problem in turbojet engines:

(1) The steady-state correlation of gas temperatures with the blade temperature in the rated-power region

(2) The dynamic-temperature characteristics (time constants) of the turbine blades at rated power, including both experimental and calculated results

(3) The gas temperature-acceleration characteristics in the starting region.

The data for the rated-power region are taken at two flight speeds and several altitudes, whereas the starting characteristics data are taken at sea level and zero ram.

APPARATUS

Engine Installation

The engine from which the data were obtained had an axial-type compressor and a single-stage turbine. The engine was mounted in an altitude test tank, and the simulated flight conditions were varied from sea-level static to an altitude of 45,000 feet and a Mach number of 0.8.

Instrumentation

Engine speed and various gas and blade temperatures were measured both in steady-state and transient operation. An instrumentation drawing of the engine (fig. 1) indicates the positions of the gas-temperature probes.

Gas temperatures. - Two methods were used to measure the gas temperatures. One method is applicable to steady-state measurements and permits the recording of the temperatures on flight recorders. The other method is applicable to transient measurements and compensates for the dynamics introduced by the mass of the thermocouple.

The steady-state method was used to measure the gas-temperature distributions at the turbine inlet, turbine outlet, and tail-pipe stations. The turbine-inlet and turbine-outlet thermocouples were in either single-point or five-point rakes, as indicated in figure 1. The tail-pipe thermocouples were all in single-point rakes. Ten tail-pipe rakes were distributed circumferentially and the average of these was read. The temperatures were recorded on a recording potentiometer.

To accurately measure the tail-pipe gas temperature during engine transients, the dynamics of the sensing thermocouples had to be considered. The tail-pipe gas thermocouples were constructed with 18-gage wire (0.040 inch diameter) in order to prevent burnout of the thermocouples. At sea-level rated-power conditions, the frequency response of these thermocouples is flat to less than 1 cycle per second, whereas for adequate information, it is necessary to read flat to at least 5 cycles per second. With altitude, the frequency response of the thermocouples becomes worse.

A compensation method, similar to that discussed in reference 5, is necessary in the measurement of transient tail-pipe gas temperature. The method used in this experimental study is shown in block diagram form in figure 2(a). The signal X entering the compensation network is, in operational form,

$$X(s) = \left[\frac{1}{1 + \tau_{tc}s}\right] T_g(s) \qquad (1)$$

where τ_{tc} is the time constant of the thermocouple. (The symbols used in this report are defined in appendix A.) If the compensation network is assumed to have the transfer function

$$E(s) = \left[1 + \tau_d s\right] X(s) \qquad (2)$$

[redacted]

where τ_d is an adjustable time constant, and if $\tau_d = \tau_{tc}$, then:

$$E(s) = T_g(s) \tag{3}$$

In practical applications, however, equation (2) is impossible to use because the derivative term introduces noise problems. A compromise must be made of the form

$$E(s) = \left[\frac{1 + \tau_d s}{1 + \gamma\tau_d s}\right] X(s) \tag{4}$$

where γ is approximately 0.1. The compensation then has increased the frequency response by a factor of ten.

The time constant of the thermocouple will change with the operating conditions and the compensation network must be adjustable. Rather than evaluate the thermocouple time constant at all conditions, the actuator shown in figure 2(b) is used to determine the proper compensation. Actuating the movable shield from an extended position to the retracted position shown in figure 2(b) imposes a step increase in gas temperature at the thermocouple. The compensation network is then adjusted to give a step increase in voltage E. One actuator and five circumferentially distributed thermocouples were used in this study. The compensated tailpipe gas temperature was recorded on a galvanometric oscillograph. The galvanometer element used had a frequency response flat to 50 cycles per second.

Turbine-blade temperatures. - The turbine-blade temperatures were measured by thermocouples which were imbedded in the turbine blades. The method of mounting the thermocouples in the blades is discussed in reference 2. The thermocouple leads were extended through the hollow rotor shaft to slip rings mounted on the front of the engine.

A steady-state survey was made of the blade temperatures with the radial array shown in figure 3(a). Two thermocouples were put on each of three of the turbine blades to obtain the six desired radial locations. The thermocouples were located at the midchord position. The steady-state turbine-blade temperatures were recorded on a recording potentiometer.

The transient data were taken with the chord-wise turbine-blade thermocouple array shown in figure 3(b). The chord section was chosen to be at the maximum radial temperature location. The dimensions of the chord-wise thermocouple locations are given in figure 3(b). Each position was duplicated to allow for thermocouple burnout. The six thermocouples were then placed two on each of three turbine blades. The transient turbine-blade temperatures were recorded on a galvanometric

oscillograph. The galvanometer elements used for recording the turbine-blade temperatures had a frequency response flat to 10 cycles per second.

Two rakes of the form shown in figure 4 were installed directly behind the turbine blades. The rakes were designed to measure the radiation from the turbine blades. Each rake had three thermocouples; one rake with the shell-type tips and one rake with the knob-type tips. The shell-type tips had a thermocouple imbedded in a black disk in order to obtain the maximum radiation sensitivity and this disk was protected by the shell to minimize the gas-temperature and wall-temperature effects upon the thermocouple reading. The knob-type tips were designed to measure a mean temperature, including blade radiation.

Only steady-state measurements made with the recording potentiometers were taken with the radiation probes.

Nozzle-diaphragm blades. - The two nozzle-diaphragm blades behind the center of each burner were instrumented with one thermocouple welded to the leading edge of each blade. The thermocouples were mounted at the midspan point of the blades. Individual measurements of the steady-state nozzle-diaphragm blade temperatures were made on a recording potentiometer.

Engine speed. - A 100-tooth tachometer-generator was mounted on an engine accessory pad and provided an electrical pulse train indicative of engine speed. The tachometer output was fed to an electronic counter which displayed the steady-state engine speed.

The electronic counter also provided a voltage signal from the pulse train which was recorded on the galvanometric oscillograph to give the transient-speed signal. The galvanometric element used had a frequency response flat to 20 cycles per second.

PROCEDURE

Steady-State Data

In order to obtain temperature profiles and distributions, steady-state data were taken at the conditions shown in table I(a). The conditions for each point were set and the following temperatures read on flight recorders: turbine inlet, nozzle-diaphragm blades, turbine blades (radial survey), turbine outlet, and tail-pipe gas temperature.

Transient Data

Transient data were taken at the conditions shown in table I(b). The initial and final engine speeds of these transients are also shown.

In the rated-power region, step increases in fuel flow corresponding to the speed changes shown in the table were supplied by a throttle plus relief-valve differential-pressure regulator assembly as discussed in reference 6. This fuel valve has a frequency response flat to over 30 cycles per second. At each condition the tail-pipe thermocouple compensator was adjusted, the step initiated, and the transients recorded on the oscillograph. Recordings were made of engine speed, turbine-blade temperatures (chord-wise survey), nozzle-diaphragm blade temperatures, and compensated tail-pipe gas temperature.

3855

In obtaining the transient runs from start to idle, the normal starting procedure for the engine was used. Three starts were recorded; a cold start, a hot start, and a normal start. Engine speed and tail-pipe gas temperature were recorded on the oscillograph.

RESULTS AND DISCUSSION

Steady-State Temperature Data

In treating the steady-state temperature-control problem, it is necessary first to evaluate the general temperature distributions throughout the engine, and second to evaluate and compare, at rated engine speed, specific gas temperature as possible control signals.

Data were taken at the steady-state conditions shown in table I(a) in order to determine the temperature distributions at various stations in the engine. The gas temperatures are plotted as functions of the distance from the outer engine wall. (The location of the thermocouples in relation to the outside wall are given in fig. 5.) These data are presented in figure 6.

The blade-temperature contour remains very similar as the operating conditions are varied, whereas the gas-temperature contours vary considerably as the conditions are varied. Therefore, measurements for at least three circumferential locations at each station were averaged for each data point presented for the turbine inlet, turbine outlet, nozzle diaphragm, and tail-pipe gas temperatures.

In order to evaluate various temperatures as possible control signals, data at actual rated engine speeds using the conditions shown in table II were taken. The maximum blade temperature is considered as a reference or base in evaluating the relative merits of the various temperatures. Since only one signal is used as the controlling signal and because the contours of the various temperature curves vary with operating condition, the average temperature value at each station was determined from the data. The variation of these average temperatures from the maximum blade temperature was then calculated and is presented in table II.

The temperature variations of the average temperatures included in table II are plotted as functions of δ/θ in figure 7. The data for these curves were taken at actual rated engine speed. The data give fairly smooth curves for the wide range of δ/θ values included in figure 7. The lower values of δ/θ indicate primarily a high altitude, and the higher values of δ/θ indicate a lower altitude. An increase in flight speed at a given altitude will increase the value of δ/θ. A value of 1.0 for δ/θ is obtained at sea-level static conditions.

The desired characteristic for a temperature-control signal has a temperature variation from the maximum blade temperature that is independent of operating conditions. In figure 7, this characteristic would be indicated by a curve independent of δ/θ, that is, a constant value of temperature differential. The deviation of the data curves in figure 7 from a constant value may be used as a measure of effectiveness of each temperature as a temperature-control signal. These curves show that tail-pipe gas temperature is the best temperature-control signal for steady-state operation. The tail-pipe gas temperature yields a negative difference of 210° F from the maximum turbine-blade temperature in the low altitude range. At altitudes above 30,000 feet ($\delta/\theta \approx 0.40$), this tail-pipe temperature differential drops to less than 200° F. The current practice of using the tail-pipe gas temperature as a temperature-control signal is therefore valid.

Turbine-Blade Temperature Dynamics

The mass of the turbine blade prevents the turbine-blade temperature from immediately following a change in the surrounding gas temperature. Analytical and experimental results in reference 3 show that the response of blade temperature to a step in gas temperature very closely approximates a first-order lag, and the dynamics of the turbine-blade temperature may be characterized by time constants. These blade dynamics allow short burst of high gas temperature without overtemperaturing the turbine blades. Reference 3 included experimental blade-temperature-dynamic data, but only at sea-level static conditions. An extension of the experimental data to a range of altitudes was desired in this investigation.

Experimental data. - Data were taken at the conditions shown in table I(b) in order to determine the blade-temperature-dynamic characteristics. The desired frequency responses were obtained by the method of reference 7. The frequency responses determined were the leading-edge, midchord, and trailing-edge turbine-blade temperature responses relative to the compensated tail-pipe gas temperature, and the compensated tail-pipe gas temperature and engine-speed responses relative to the fuel flow.

[redacted]

The responses obtained at an altitude of 7000 feet and at Mach 0.8 for a transient in engine speed from 90 to 100 percent of rated are shown in figure 8. The frequency-response curves for the transient data taken at the remainder of the conditions of table I(b) were similar in shape to the curves of figure 8.

The dynamic responses obtained at all the conditions may be closely approximated by the following transfer functions:

$$\frac{T_b}{T_g} = \frac{1}{(1 + \tau_b s)}$$

$$\frac{N}{w_f} = \frac{1}{(1 + \tau_e s)}$$

$$\frac{T_g}{w_f} = \left(\frac{1 + b\tau_e s}{1 + \tau_e s}\right)$$

The dynamic temperature characteristics of the turbine blade and tail-pipe gas temperatures are determined by the blade time constant τ_b, the engine time constant τ_e, and the tail-pipe gas temperature-rise ratio b. From plots similar to those of figure 8, the dynamic characteristics τ_b, τ_e, and b were determined for each condition investigated.

The dynamic characteristics are plotted as a function of altitude in figure 9. As shown in these curves, the turbine-blade time constants and the engine time constant increase with altitude, whereas the tail-pipe gas temperature-rise ratio decreases as the altitude increases.

Use in control. - If $\tau_b > b\tau_e$ and if in a transient, the engine speed never overshoots the final speed, the blade temperature will never overshoot its final value. This characteristic is of particular importance at the rated engine power condition, where blade overtemperature can damage the blades. For the engine studied in this report, the ratio $\tau_b/b\tau_e$ is greater than unity in the region above 8000 feet at Mach 0.8 and rated engine power. In this operating region then, a speed control which permits no speed overshoot will prevent any overshoot in turbine-blade temperature and eliminates the need for a separate temperature-limiting control.

Analytical development. - The study presented herein will include the calculation of the film coefficients for the midchord and trailing-edge portions of the turbine blade, the calculation of the turbine-blade temperature dynamic responses, and the calculations of the variation of the dynamic responses with altitude.

Two analytical methods of determining the dynamic response of turbine-blade temperature to tail-pipe gas temperature were presented in reference 3 and are used in this study. In one method (method A) only the lag due to the film coefficient is considered, whereas in the other method (method B) the temperature gradient within the blade is also considered. For thin cross sections, such as turbine blades, method A and method B yield very similar results. Method A yields directly a time constant, and the results of method B may be characterized by a time constant.

The calculations for the film coefficient h for the midchord and trailing-edge portions of the turbine blade are presented in detail in appendix B. These calculations are based on information given in references 4, 8, and 9. A scale drawing of the blade is shown in figure 10, and the shapes assumed for the portions of the blade used in calculations are superimposed. The conditions for which the calculations were made are rated engine speed, an altitude of 7000 feet, and a Mach number of 0.8. The results of the film-coefficient calculations are included in table III.

The dynamic responses of the turbine-blade temperature to the tail-pipe gas temperature were calculated for the midchord and trailing-edge portions of the turbine blade. These calculations are presented in detail in appendix C, and the results of the calculations included in table III. No attempt was made to calculate either the film coefficient or the time constant of the leading-edge portion of the blade because of insufficient knowledge of the heat-transfer characteristics of this portion of the blade.

The results of the calculations, in the form of frequency responses, are presented in figure 11. Because of the thin turbine blade considered, methods A and B gives very similar results in the midchord and trailing-edge regions.

The variations of the turbine-blade time constants with altitude are calculated in appendix D. The time constants were found to vary inversely with $w_a^{0.8}$, which means the time constants increase as the altitude increases. A curve of $(1/w_a)^{0.8}$ as a function of altitude for the engine investigated is shown in figure 12.

Correlation of experimental and analytical results. - The blade time-constant calculations, summarized in table III were made for a condition at Mach 0.8, an altitude of 7000 feet, and at an actual rated engine speed. A comparison of the experimental values with the calculated values is made in table III, and good agreement is obtained.

As developed in appendix C, the blade time-constant variation with altitude was inversely as $w_a^{0.8}$. The comparison of the calculated curve

with the experimental data is made in figure 12. All curves shown were normalized with the values at 7000 feet used as the base values. Good agreement is obtained between the experimental and calculated variations.

Gas Temperature and Acceleration Characteristics in Starting Region

Transient measurements of several engine starts were taken, and these records were analyzed to give tail-pipe gas temperature, engine speed, and engine acceleration. Gas temperature is plotted against engine speed with lines of constant acceleration in figure 13. The plot shows that at each engine speed there is a maximum acceleration. The path a maximum acceleration transient should take is represented by the dashed line. Increasing the tail-pipe gas temperature above that corresponding to the maximum acceleration decreases the acceleration value at the corresponding engine speed.

Therefore, a maximum acceleration for this engine may be obtained over the majority of the start-to-idle speed range with tail-pipe gas temperatures below 1400° F.

CONCLUDING REMARKS

A correlation was made between the maximum blade temperature and various average gas temperatures in order to determine an applicable steady-state temperature control signal. Ideally, this temperature signal would indicate the maximum blade temperature at all flight speeds and altitudes.

The most applicable temperature signal found was the commonly used tail-pipe gas temperature. For the engine studied, the tail-pipe gas temperature gave a constant 210° F differential below the maximum blade temperature at low altitudes, which decreased to 180° F at high altitudes.

The dynamic responses of the turbine-blade temperatures to the tail-pipe gas temperatures at actual rated engine speed were evaluated over a range of altitudes. For all conditions, the dynamic responses were found to be essentially first-order lags. For this reason, the blade temperature dynamic response may be represented by a characteristic time constant. These blade time constants vary with position on the blade, the leading edge having the shortest time constant, the trailing edge slightly longer, and the midchord time constant longer than the leading-edge time constant by a factor of approximately two.

[redacted]

The time constants for the trailing edge, and midchord portions of the turbine blade were calculated and showed good agreement with the experimental results.

The time constants increased with an increase in altitude, and this variation correlated very well with a theoretical calculated variation. The calculated variation indicated that the blade time constants varied inversely as $w_a^{0.8}$.

For the engine studied, at conditions of an altitude above 8000 feet and Mach 0.8, at rated engine speed, the turbine-blade time constants were larger than the product of the tail-pipe gas temperature-rise ratio and the engine time constant. With this condition, a speed control that permits no speed overshoot will prevent any overshoot in turbine-blade temperature and will eliminate the need for a separate temperature-limiting control.

At each engine speed during the transient from start to idle, there was a definite maximum acceleration obtainable. Over the majority of the start-to-idle speed range, this maximum occurred at a tail-pipe gas temperature of less than 1400° F for the engine studied.

Lewis Flight Propulsion Laboratory
National Advisory Committee for Aeronautics
Cleveland, Ohio, January 4, 1956

APPENDIX A

SYMBOLS

A	wetted area of turbine blade section, sq ft
a	blade thickness of chord section of turbine blade, in.
b	tail-pipe gas temperature-rise ratio
C	constant
c_p	specific heat of turbine-blade material, Btu/(lb)(°F)
D	characteristic dimension, ft
E	output voltage of tail-pipe gas temperature compensation network, v
h	film coefficient, Btu/(hr)(°F)(ft)
K	proportionality constant, h/k, $in.^{-1}$
k	gas conductivity, Btu/(hr)(°F)(ft)
M	Mach number
N	engine rotor speed, rpm
Nu	Nusselt number
Pr	Prandtl number
Re	Reynolds number
s	complex Laplacian operator
T	temperature, °F or °R
t	time, sec
V	volume of turbine-blade section, cu ft
v	gas velocity, ft/sec
w_a	engine air flow, lb/sec

w_f engine fuel flow, lb/sec

x tail-pipe gas temperature signal to compensation network, v

α diffusivity of blade material, $\sqrt{\frac{(ft)(in.)}{hr}}$

γ reciprocal of rise ratio of compensation network

δ ratio of absolute total pressure at engine inlet to NACA standard atmospheric pressure at sea-level static conditions

θ ratio of absolute total temperature at engine inlet to NACA standard atmospheric temperature at sea-level static conditions

ν kinematic viscosity of gas, sec/sq ft

ρ_b density of turbine blade, lb/cu ft

τ turbine-blade time constant for response to tail-pipe gas temperature, sec

τ_d time constant of compensation network, sec

τ_e engine time constant, sec

τ_{tc} time constant of tail-pipe gas measuring thermocouples, sec

Ω break frequency of first-order lag frequency plots, radians/sec

ω angular frequency, radians/sec

Subscripts:

b turbine blade

e engine

g tail-pipe gas

i turbine inlet

l leading edge of turbine blade

m midchord of turbine blade

n nozzle diaphragm

[redacted]

o	turbine outlet
p	pressure side of turbine blade
s	suction side of turbine blade
sh	shell-type radiation probe
t	trailing edge of turbine blade
x,y	arbitrary altitude conditions

APPENDIX B

CALCULATION OF FILM COEFFICIENTS

In calculating the dynamic responses of turbine-blade temperature to tail-pipe gas temperature, a determination of the appropriate value of the heat-transfer film coefficient for each position considered in the turbine blade is necessary. The film coefficients are dependent on the shape of the blade and the properties of the gas at the condition being considered.

The film coefficients for the midchord and trailing-edge portions of the blade were calculated using the method suggested in reference 4. No attempt was made to calculate either the film coefficient or the time constant of the leading-edge portion of the blade because of insufficient knowledge of the heat-transfer characteristics of this portion of the blade.

The gas conditions used in the calculations presented herein are listed in table IV. The velocity distribution determined by the method of reference 10 is shown in figure 14. The calculations are at actual rated engine speed, an altitude of 7000 feet, and Mach 0.8

Midchord Film Coefficient

The midchord thermocouple is considered to be at the midthickness of a rectangular section which is 1.15 inches from the leading edge of the blade as shown in figure 10. The calculation for the film coefficient must be carried out in two parts, one for the suction surface and the other for the pressure surface.

Suction surface. - The flow is turbulent and the applicable equation is:

$$Nu = 0.0296(Re)^{0.8}Pr^{1/3} \qquad (B1)$$

where

$$Re = \frac{D_{m,s}V\rho}{\mu} = \left(\frac{1.28}{12}\right)(1530)\left(\frac{10^5}{150} \times \frac{6100}{2117}\right) = 31.5\times10^4$$

$$Nu = \frac{h_{m,s}D_{m,s}}{k} = h_{m,s}\left(\frac{1.28}{12}\right)\left(\frac{1}{0.0451}\right) = 2.37h_{m,s}$$

$$Pr = 0.655$$

[redacted]

Solving equation (B1) gives:

$$h_{m,s} = 276 \text{ Btu/(hr)(°F)(sq ft)}$$

Pressure surface. - The negative velocity gradient for the pressure surface in the midchord region indicates turbulent flow and equation (B1) is again applicable. In this case:

$$\text{Re} = \frac{D_{m,p} v \rho}{\mu} = \left(\frac{1.05}{12}\right)(416)\left(\frac{10^5}{150} \times \frac{6100}{2117}\right) = 7.0 \times 10^4$$

$$\text{Nu} = \frac{h_{m,p} D_{m,p}}{k} = h_{m,p}\left(\frac{1.05}{12}\right)\left(\frac{1}{0.0451}\right) = 1.94 h_{m,p}$$

$$\text{Pr} = 0.655$$

Solving equation (B1) gives:

$$h_{m,p} = 102.6 \text{ Btu/(hr)(°F)(sq ft)}$$

Trailing-Edge Film Coefficient

As shown in figure 10, the trailing-edge thermocouple is considered to be at the midthickness of a rectangular section which is 2.15 inches from the leading edge of the blade. The velocity on the pressure surface in the trailing-edge region is approximately 700 feet per second, as taken from figure 14. For the calculations presented herein, it will be assumed that the velocity on the suction surface in the trailing-edge region is also 700 feet per second, that the flow is turbulent, and that there is no flow separation in this region.

The film coefficient may again be obtained from equation (B1).

$$\text{Re} = \frac{D_t v \rho}{\mu} = \left(\frac{2.15}{12}\right)(700)\left(\frac{10^5}{150} \times \frac{6100}{2117}\right) = 24.2 \times 10^4$$

$$\text{Nu} = \frac{h_t D_t}{k} = h_t\left(\frac{2.15}{12}\right)\left(\frac{1}{0.0451}\right) = 3.97 h_t$$

$$\text{Pr} = 0.655$$

and solving equation (B1) gives:

$$h_t = 128 \text{ Btu/(hr)(°F)(sq ft)}$$

[redacted]

APPENDIX C

CALCULATION OF TURBINE-BLADE TEMPERATURE DYNAMIC RESPONSE

Two methods of determining the dynamic response of turbine-blade temperature to tail-pipe gas temperature were presented in reference 3. Both methods involve the physical properties of the blade and the film coefficients. The blade properties are known and the film coefficients are calculated in appendix B.

Method A

Method A assumes that the temperature is equal throughout the blade and that the heat flow is proportional to the difference in temperature between the gas and the turbine blade. The general form of the dynamic response of the blade temperature, using Method A, is (from ref. 3)

$$\frac{V_b \rho_b c_p}{h_b A_b} \frac{dT_b}{dt} + T_b = T_g \tag{C1}$$

As this equation is a first-order differential equation, it can be characterized by a time constant which is defined as

$$\tau_b \triangleq \frac{V_b \rho_b c_p}{h_b A_b} \tag{C2}$$

As discussed in reference 3, equation (C1) may be converted to the frequency domain by Laplacian transform methods and yields

$$\frac{T_b}{T_g} = \frac{1}{(1 + i\omega\tau_b)} \tag{C3}$$

The plots of figure 11 are frequency response plots of equation (C3), where τ_b is the blade time constant determined from Method A.

Midchord. - The midchord is considered to be a rectangular section (fig. 10). The calculation of the midchord time constant is (considering h_m as the average of the pressure and suction surface value)

$$\tau_m = \left(\frac{V_m}{A_m}\right)\left(\frac{1}{h_m}\right)(\rho_b c_p) = \left(\frac{0.15}{24}\right)\left(\frac{1}{189}\right)(59.4) \tag{C4}$$

which gives as a final result

$$\tau_m = 7.06 \text{ seconds}$$

Trailing edge. - The trailing edge is also considered to be a rectangular section (fig. 10). The calculation of the trailing-edge time constant is

$$\tau_t = \left(\frac{V_t}{A_t}\right)\left(\frac{1}{h_t}\right)(\rho_b c_p) = \left(\frac{0.06}{24}\right)\left(\frac{1}{128}\right)(59.4) \tag{C5}$$

which gives as a final result

$$\tau_t = 4.17 \text{ seconds}$$

Method B

This method is the more rigorous because the temperature gradient in the turbine blade is considered. The solution for the rectangular shaped midchord and trailing-edge portions of the turbine blade is developed in reference 3 from the heat-transfer equation

$$\nabla^2 T_b = \frac{1}{\alpha^2}\frac{\partial T_b}{\partial t} \tag{C6}$$

and appropriate boundary conditions. The solution is

$$\frac{T_b}{T_g} = \frac{1}{\frac{\sqrt{i\omega}}{aK}\sinh\left(\frac{a\sqrt{i\omega}}{2\alpha}\right) + \cosh\left(\frac{a\sqrt{i\omega}}{2\alpha}\right)} \tag{C7}$$

Each term of the denominator may be represented in series form as

$$\frac{\sqrt{i\omega}}{aK}\sinh\left(\frac{a\sqrt{i\omega}}{2\alpha}\right) = \frac{\sqrt{i\omega}}{aK}\left\{\left(\frac{a\sqrt{i\omega}}{2\alpha}\right) + \frac{1}{3!}\left(\frac{a\sqrt{i\omega}}{2\alpha}\right)^3 + \cdots\right. \tag{C8}$$

$$\cosh\left(\frac{a\sqrt{i\omega}}{2\alpha}\right) = 1 + \frac{1}{2!}\left(\frac{a\sqrt{i\omega}}{2\alpha}\right)^2 + \frac{1}{4!}\left(\frac{a\sqrt{i\omega}}{2\alpha}\right)^4 + \cdots \tag{C9}$$

Since the frequency ω is considerably less than unity in the region of interest, only the ω and ω^2 terms will be considered. This gives then, for the dynamic response of turbine-blade temperature to the tailpipe gas temperature

[redacted]

$$\frac{T_b}{T_g} = \frac{1}{1 + i\omega\left\{\frac{1}{\alpha K}\left(\frac{a}{2\alpha}\right) + \frac{1}{2}\left(\frac{a}{2\alpha}\right)^2\right\} + \omega^2\left\{-\frac{1}{6\alpha K}\left(\frac{a}{2\alpha}\right)^3 - \frac{1}{24}\left(\frac{a}{2\alpha}\right)^4\right\}} \quad (C10)$$

The ω^2 term is a second-order effect, and from equation (C10)

$$\tau_b \cong \frac{1}{\alpha K}\left(\frac{a}{2\alpha}\right) + \frac{1}{2}\left(\frac{a}{2\alpha}\right)^2 \quad (C11)$$

The time constant of Method A, in the same units, is

$$\tau_b = \frac{1}{\alpha K}\left(\frac{a}{2\alpha}\right) \quad (C12)$$

and Method B, as expected, increases the time constant, approximately by the term $\frac{1}{2}\left(\frac{a}{2\alpha}\right)^2$. This term is a property of the blade only and results from the consideration of the temperature gradient with the blade. As the thickness a becomes very small, the two methods will yield the same answer.

Midchord. - The values for the midchord section which are substituted into equation (C10) are

$$\alpha = \sqrt{\frac{k}{c_p \rho_b}} = 0.0934 \text{ in./}\sqrt{\text{sec}}$$

$$K = \frac{h_m}{k} = 1.22 \text{ in.}^{-1}$$

$$\frac{a_m}{2} = 0.075 \text{ in.}$$

The solution of equation (C10) for the midchord section is plotted in figure 11(a), and a time constant of 7.25 seconds is obtained.

Trailing edge. - The values for the trailing-edge section which are substituted into equation (C10) are

$$\alpha = \sqrt{\frac{k}{c_p \rho_b}} = 0.0934 \text{ in.}/\sqrt{\text{sec}}$$

$$K = \frac{h_t}{k} = 0.826 \text{ in.}^{-1}$$

$$\frac{a_t}{2} = 0.03 \text{ in.}$$

The solution of equation (C10) for the trailing-edge section is plotted on figure 11(b), and a time constant of 4.17 seconds is obtained.

3855

[redacted]

APPENDIX D

CALCULATION OF DYNAMIC RESPONSE VARIATION WITH ALTITUDE

The time constants for the leading-edge, midchord, and trailing-edge portions of the turbine blade are dependent upon the physical properties of the blade and the film coefficient between the blade and the gas stream. Since only the film coefficient varies with altitude, the relation

$$\tau_b \propto \frac{1}{h} \tag{D1}$$

may be used in determining altitude effects upon the blade time constant. All three portions of the blade considered had turbulent flow, and the general equation

$$Nu = C(Re)^{0.8} \tag{D2}$$

will hold in the range of Reynolds number encountered. Equation (D2) may be rewritten:

$$\frac{(Nu)_x}{(Nu)_y} = \frac{C_x(Re_x)^{0.8}}{C_y(Re_y)^{0.8}} \tag{D3}$$

where x and y are two altitude conditions. The constants C_x and C_y are equal, and expanding equation (3) gives

$$\left(\frac{h_x D_x}{k_x}\right)\left(\frac{k_y}{h_y D_y}\right) = \left(\frac{V_x \rho_x D_x}{\mu_x}\right)^{0.8}\left(\frac{\mu_y}{V_y \rho_y D_y}\right)^{0.8} \tag{D4}$$

Assuming a constant turbine-inlet temperature

$$\frac{h_x}{h_y} = \left(\frac{V_x \rho_x}{V_y \rho_y}\right)^{0.8} = \left(\frac{w_{a,x}}{w_{a,y}}\right)^{0.8} \tag{D5}$$

which in terms of the blade time constants is

$$\frac{\tau_x}{\tau_y} = \left(\frac{w_{a,x}}{w_{a,y}}\right)^{0.8} \tag{D6}$$

REFERENCES

1. Farmer, J. Elmo: Relation of Nozzle-Blade and Turbine-Bucket Temperatures to Gas Temperatures in a Turbojet Engine. NACA RM E7L12, 1948.

2. Morse, C. R., and Johnston, J. R.: Temperatures in a J47-25 Turbojet-Engine Combustor and Turbine Sections During Steady-State and Transient Operation in a Sea-Level Test Stand. NACA RM E54K30a, 1955.

3855

3. Hood, Richard, and Phillips, William E., Jr.: Dynamic Response of Turbine-Blade Temperature to Exhaust-Gas Temperature for Gas-Turbine Engines. NACA RM E52A14, 1952.

4. Schafer, Louis J., Jr., Stepka, Francis S., and Brown, W. Byron: Comparison of Theoretically and Experimentally Determined Effects of Oxide Coatings Supplied by Fuel Additives on Uncooled Turbine-Blade Temperature During Transient Turbojet-Engine Operation. NACA RM E53A19, 1953.

5. Shepard, Charles E., and Warshawsky, Isidore: Electrical Techniques for Compensation of Thermal Time Lag of Thermocouples and Resistance Thermometer Elements. NACA TN 2703, 1952.

6. Otto, Edward W., Gold, Harold, and Hiller, Kirby W.: Design and Performance of Throttle-Type Fuel Controls for Engine Dynamic Studies. NACA TN 3445, 1955.

7. LaVerne, Melvin E., and Boksenbom, Aaron S.: Frequency Response of Linear Systems from Transient Data. NACA Rep. 977, 1950. (Supersedes NACA TN 1935.)

8. Eckert, E. R. G.: Introduction to the Transfer of Heat and Mass. McGraw-Hill Book Co., Inc., 1950.

9. Hubbartt, James E., and Schum, Eugene F.: Average Outside-Surface Heat-Transfer Coefficients and Velocity Distributions for Heated and Cooled Impulse Turbine Blades in Static Cascades. NACA RM E50L20, 1951.

10. Delio, Gene J., and Rosenzweig, Solomon: Dynamic Response at Altitude of a Turbojet Engine with Variable Area Exhaust Nozzle. NACA RM E51K19, 1952.

[redacted]

TABLE I. - PERFORMANCE CONDITIONS

(a) Steady state

Altitude, ft	Mach number	Engine speed, percent	Engine-inlet pressure, lb/sq ft	Engine-inlet temperature, °R
7,000	0.5	100	1935	519
	.8	100	2490	557
15,000	0.8	100	1821	525
25,000	0.5	100	931	451
	.8	100	1197	485
30,000	0.5	100	745	432
	.8	100	958	464
45,000	0.5	100	365	411
	.8	100	470	442

(b) Transient

Altitude, ft	Mach number	Engine speed, percent
Sea level	0	Start to idle
7,000	.8	90-100
15,000	.8	90-100
25,000	.8	90-100
45,000	.8	90-100

[redacted]

TABLE II. - STEADY-STATE TEMPERATURE DISTRIBUTIONS AT VARIOUS OPERATING CONDITIONS AT RATED ENGINE SPEED

Altitude, ft	Mach number	Inlet pressure, lb/sq ft	Inlet temperature, °R	δ/θ	Maximum blade temperature, T_b, °F	$T_i - T_b$, °F	$T_n - T_b$, °F	$T_{sh} - T_b$, °F	$T_o - T_b$, °F	$T_g - T_b$, °F	$\frac{T_i - T_o}{2} - T_b$, °F
7,000	0.5	1938	519	0.917	1425	255	135	-140	-165	----	45
	.8	2490	557	1.095	1415	225	120	-135	-180	-220	23
15,000	0.8	1821	525	0.850	1415	275	150	-125	-165	-205	55
25,000	0.5	931	451	0.606	1420	290	170	-95	-160	----	65
	.8	1197	485	.605	1400	295	172	-110	-160	-205	67
30,000	0.5	745	432	0.424	1425	290	165	-105	-160	-205	55
	.8	958	464	.505	1400	280	170	-90	-155	-195	62
45,000	0.5	365	411	0.218	1480	255	160	-70	-135	-175	60
	.8	470	470	.260	1395	275	165	-70	-155	-200	60

TABLE III. - EXPERIMENTAL AND CALCULATED TURBINE DYNAMIC CHARACTERISTICS. ALTITUDE, 7000 FEET; MACH NUMBER, 0.8; PERCENT RATED ENGINE SPEED, 90 TO 100

Blade section	Experimental time constant, τ_b, sec	Calculated time constant, τ_b, sec		Calculated film coefficient, h_b, Btu/(hr)(°F)(ft)
		Method A	Method B	
Leading edge	3.25	----	----	----------
Midchord	6.70	7.06	7.25	Pressure surface, 102.6 Suction surface, 276
Trailing edge	3.50	4.17	4.17	128

TABLE IV. - GAS CONDITIONS USED FOR CALCULATIONS

[Altitude, 7000 feet.]

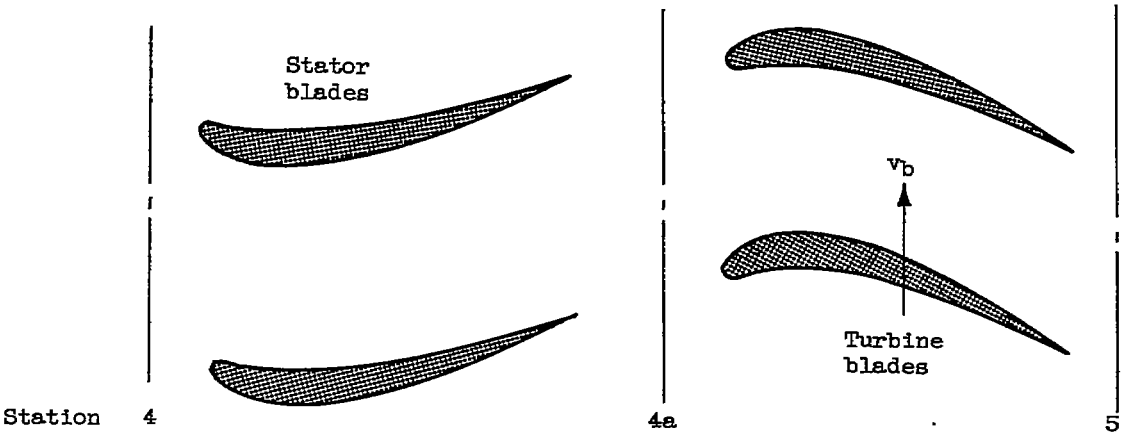

	Engine inlet	Station 4	Station 4a	Relative to turbine blades
Mach number	0.8	------	1.0	0.68
Total pressure, lb/sq ft	2490	11,580	11,580	8320
Static pressure, lb/sq ft	----	------	6100	6100
Total temperature, ^{o}R	----	2160	2160	1965
Static temperature, ^{o}R	----	----	1800	1800
Velocity, ft/sec	----	----	2050	1395

[redacted]

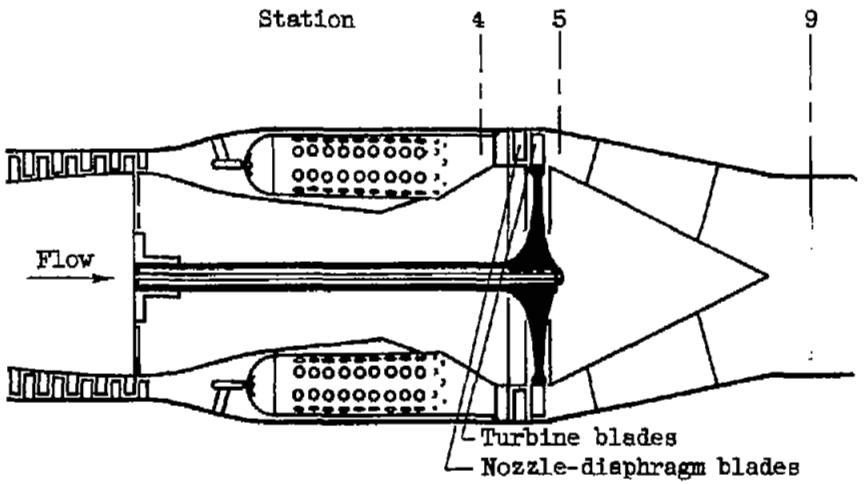

(a) Cross section of engine.

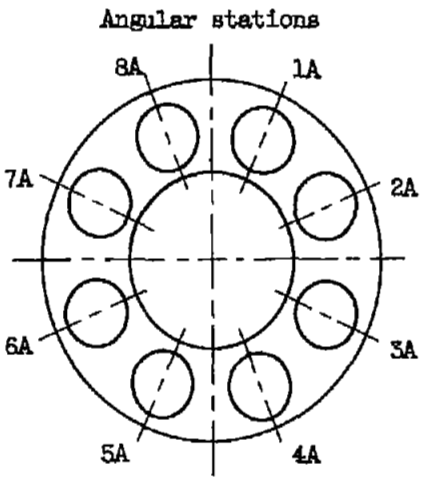

(b) Burner section.

Turbine outlet (station 5)	Turbine inlet (station 4)	Tail pipe (station 9)	Nozzle diaphragm
Three 5-point thermocouple rakes (1A, 4A, 6A) Two radiation thermocouple probes (2A, 7A)	Three 5-point thermocouple rakes (1A, 4A, 6A) Four 1-point thermocouple rakes (2A, 3A, 5A, 7A)	Steady state - 10 single thermocouples in ring Transient - 5 compensated thermocouples in ring.	Two leading-edge thermocouples behind each combustor.

Figure 1. - Instrumentation drawing.

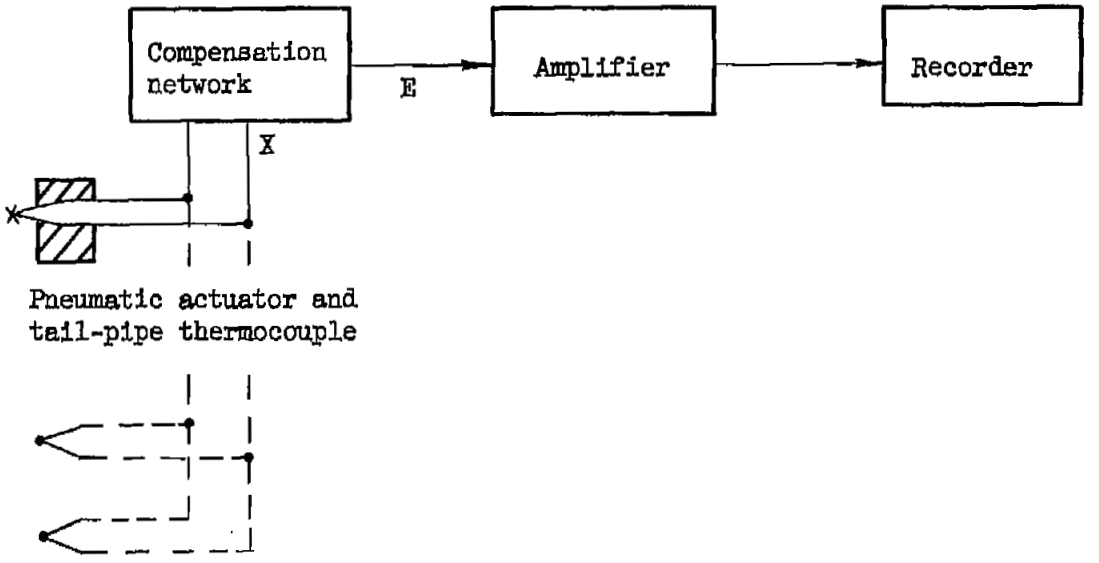

(a) Compensated gas-temperature block diagram.

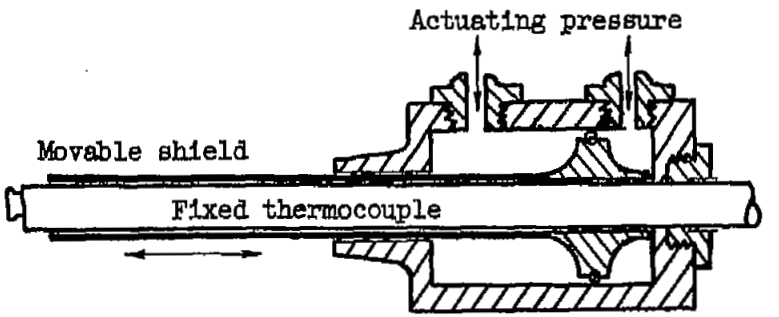

(b) Pneumatic-actuated shield assembly.

Figure 2. - Apparatus used to compensate for lag of tail-pipe thermocouples.

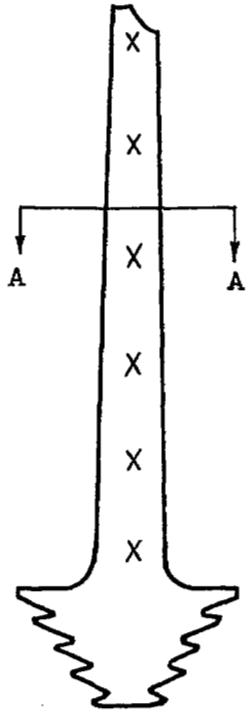

(a) Radial blade thermocouples.

X Thermocouple location

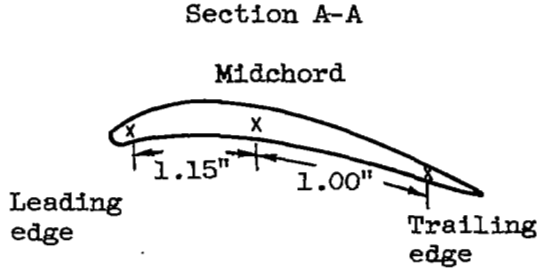

(b) Chordwise turbine-blade thermocouples.

Figure 3. - Location of both spanwise and chordwise thermocouples on turbine blade.

3855

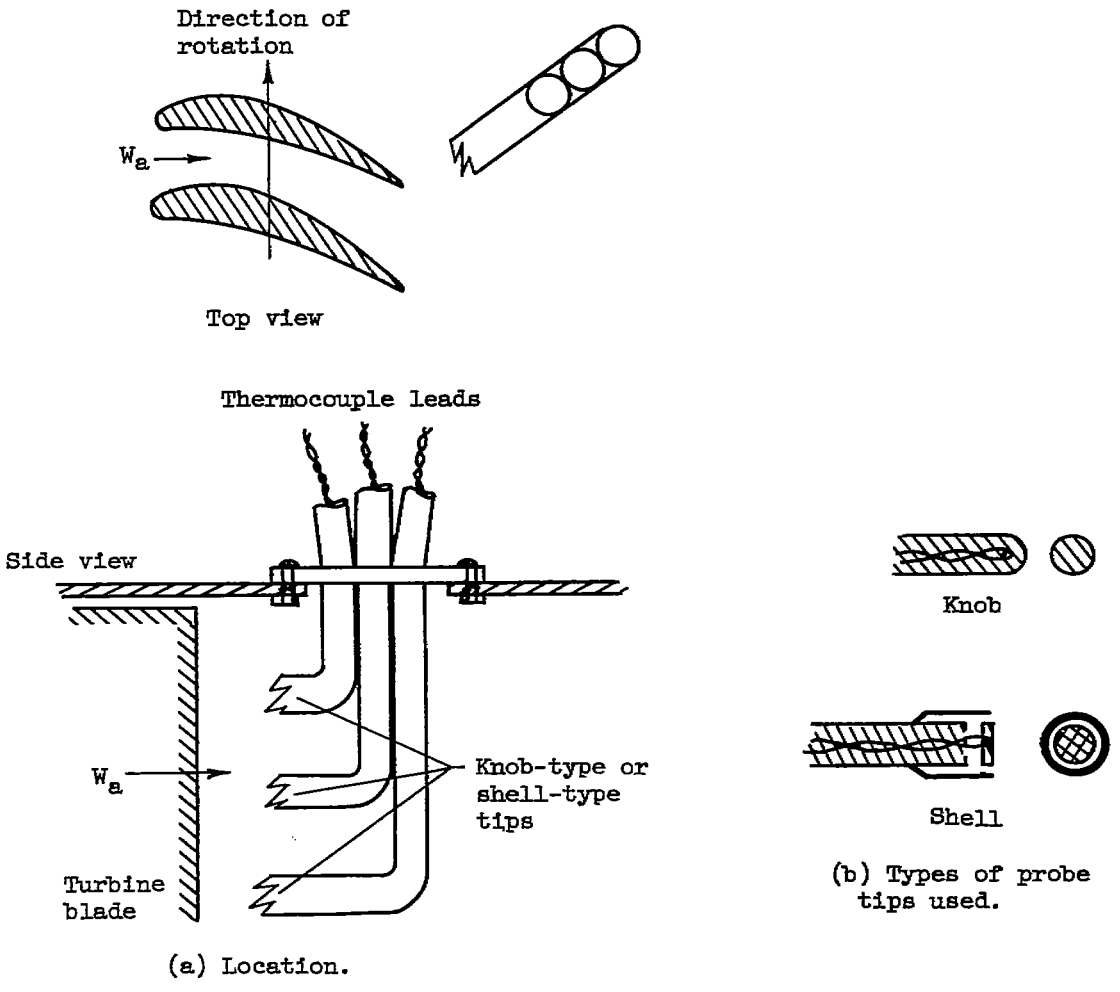

(a) Location.

(b) Types of probe tips used.

Figure 4. - Radiation probes.

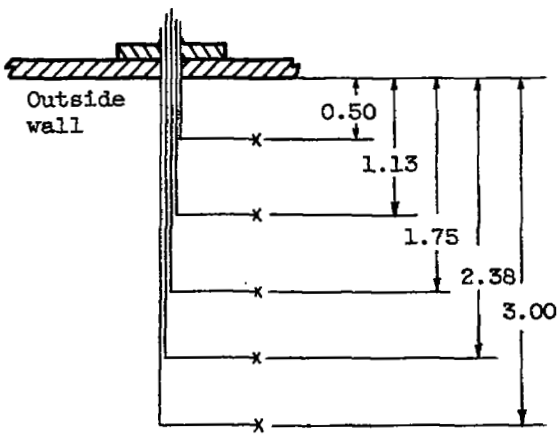

(a) Turbine inlet and outlet thermocouple rakes.

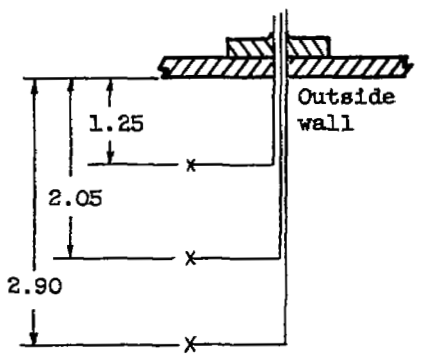

(b) Knob-type radiation probe.

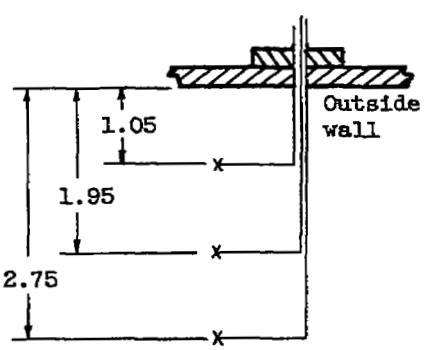

(c) Shell-type radiation probe.

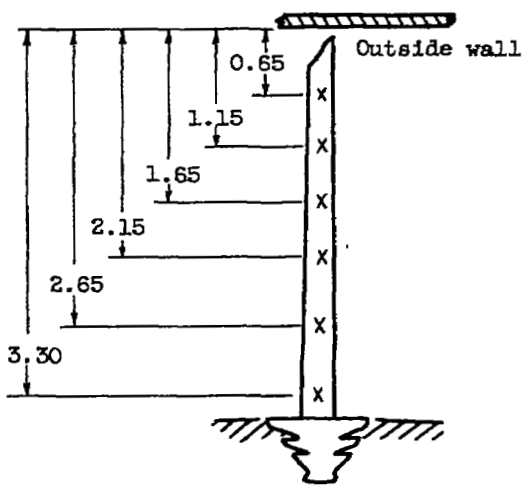

(d) Radial location of turbine-blade thermocouples.

Figure 5. - Distance from outside wall for various thermocouples. (All dimensions in inches.)

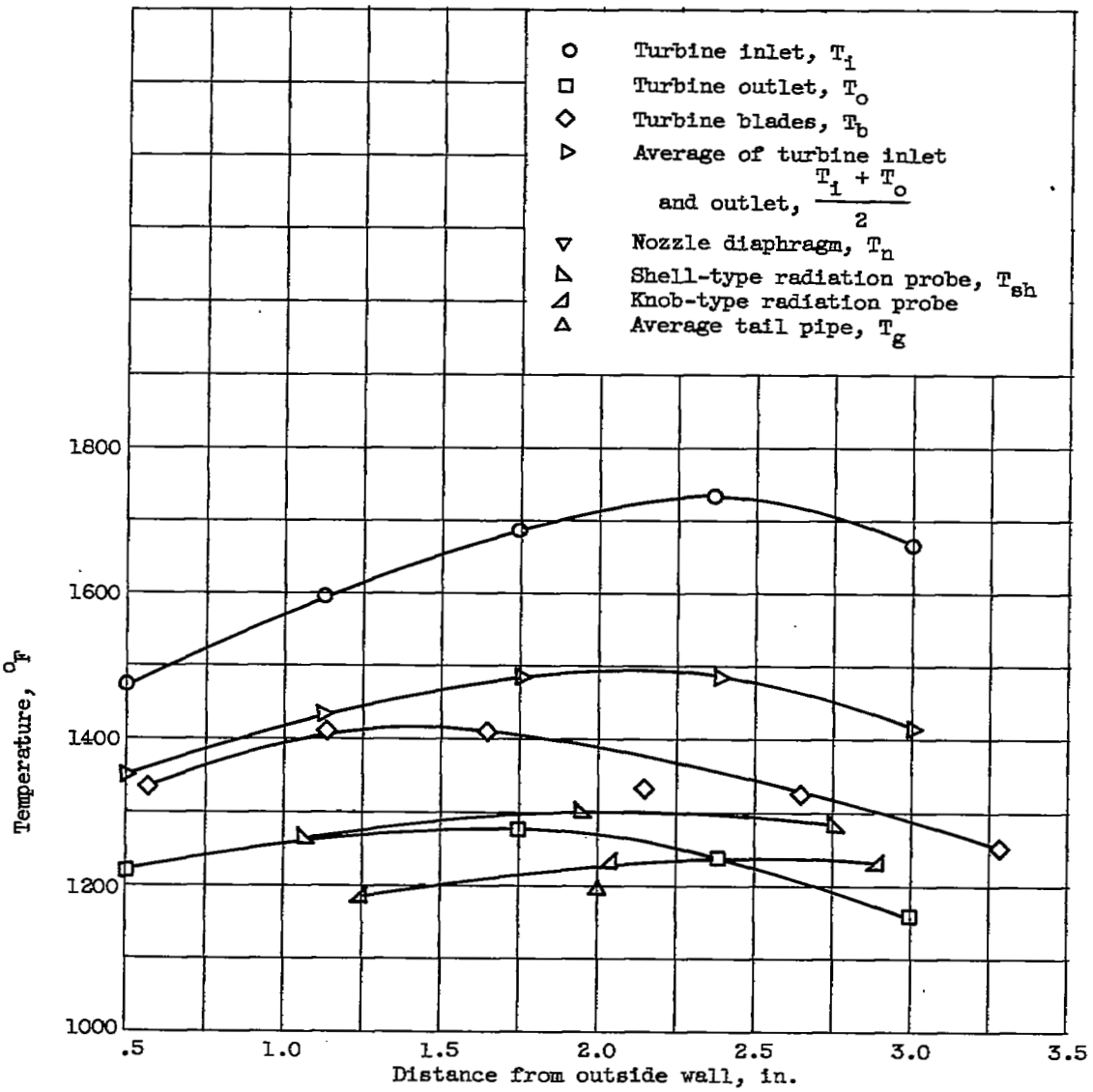

(a) Altitude, 7000 feet.

Figure 6. - Steady-state temperature distribution. Mach number, 0.8; rated engine speed.

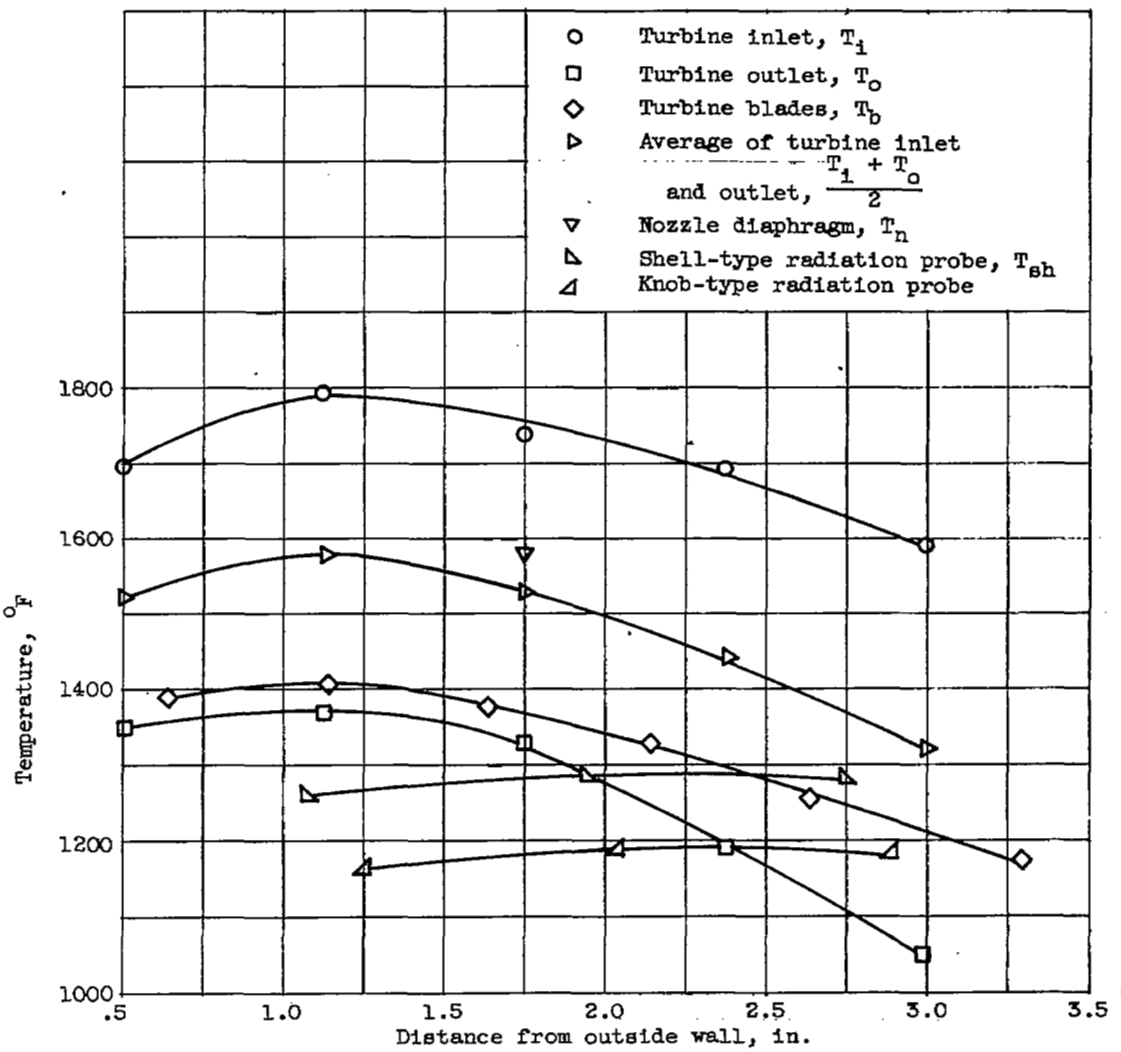

(b) Altitude, 25,000 feet.

Figure 6. - Continued. Steady-state temperature distribution. Mach number, 0.8; rated engine speed.

[redacted]

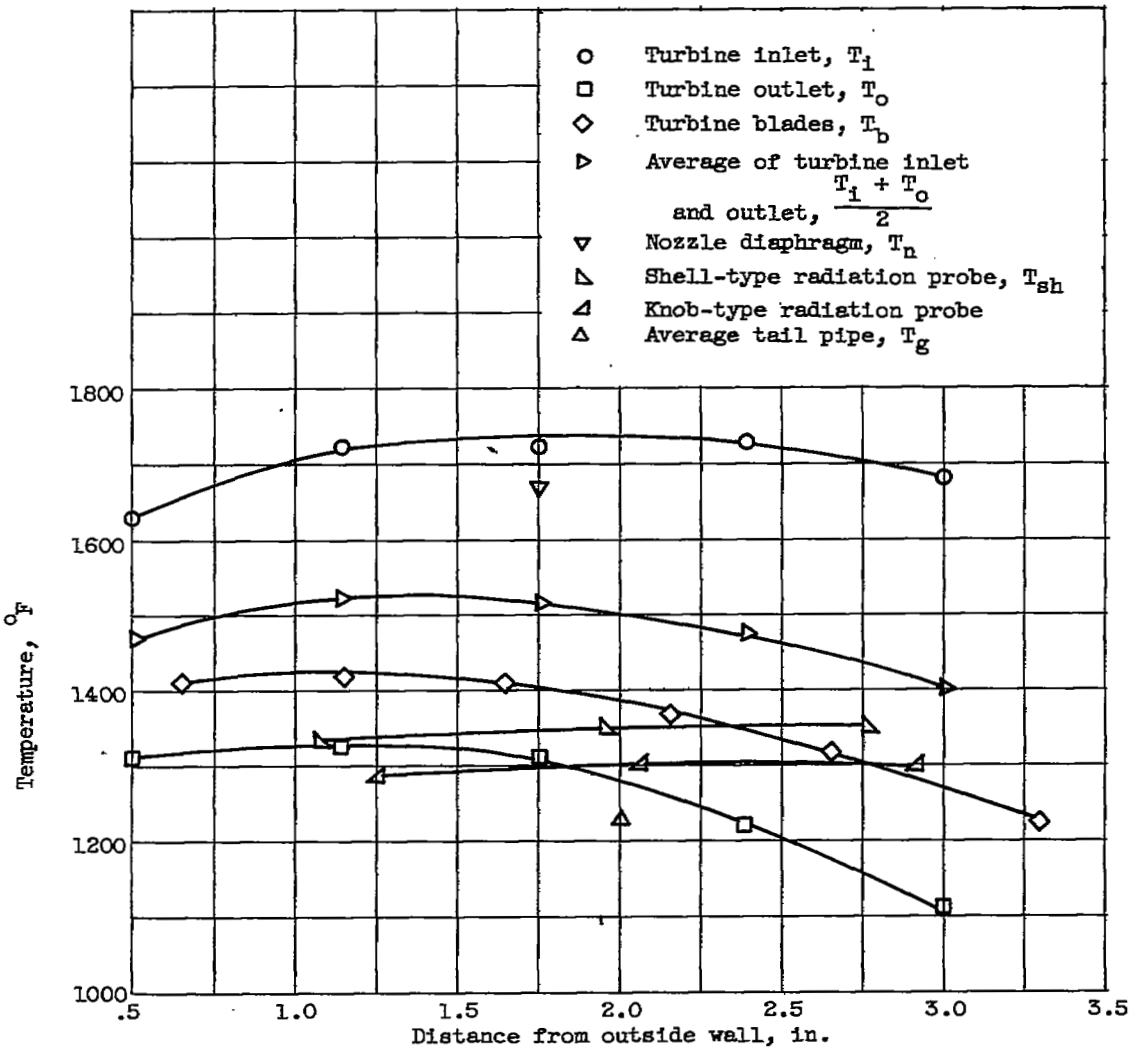

(c) Altitude, 45,000 feet.

Figure 6. - Concluded. Steady-state temperature distribution. Mach number, 0.8; rated engine speed.

[redacted]

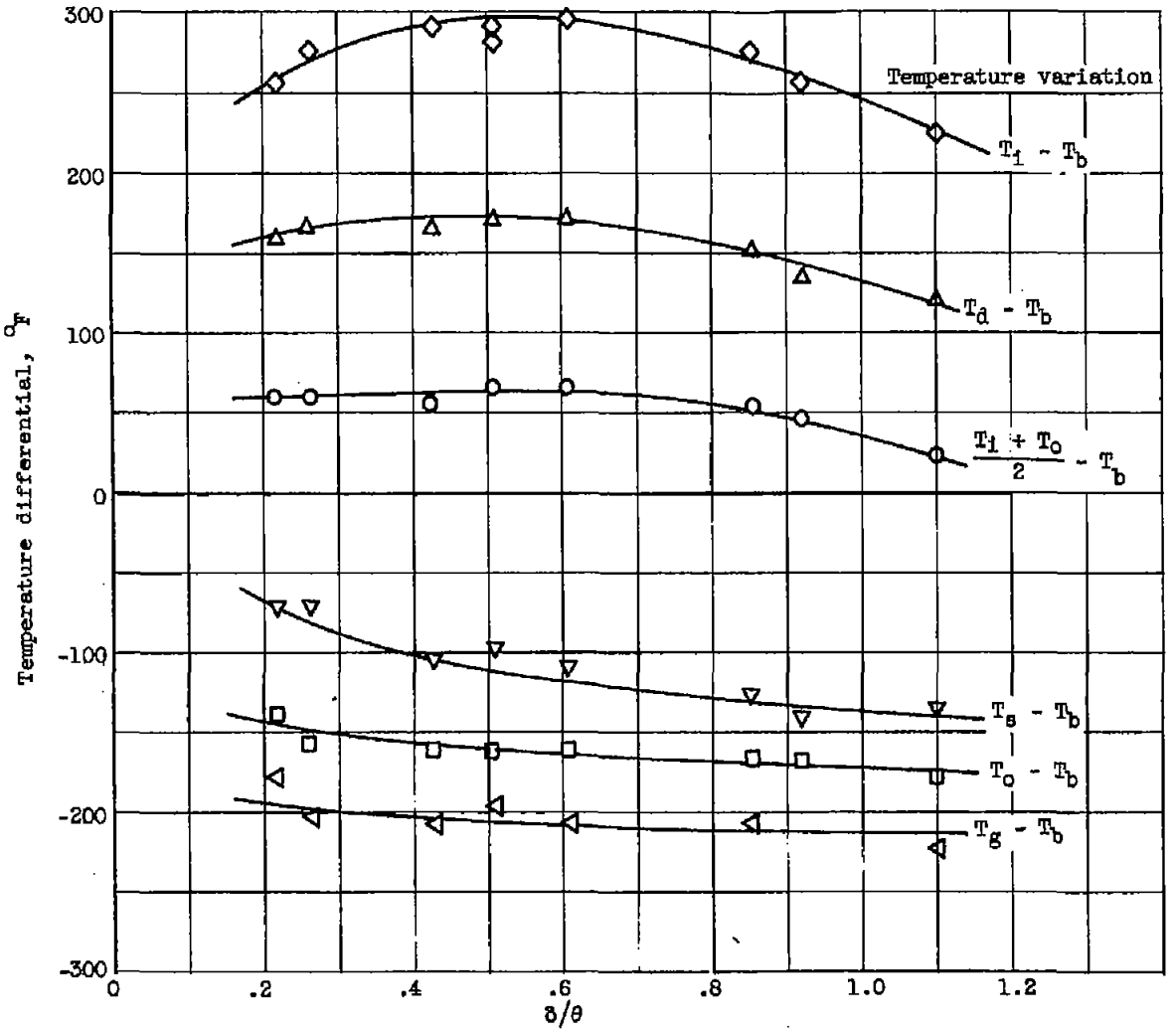

Figure 7. - Steady-state temperature levels as functions of operating conditions. Rated engine speed.

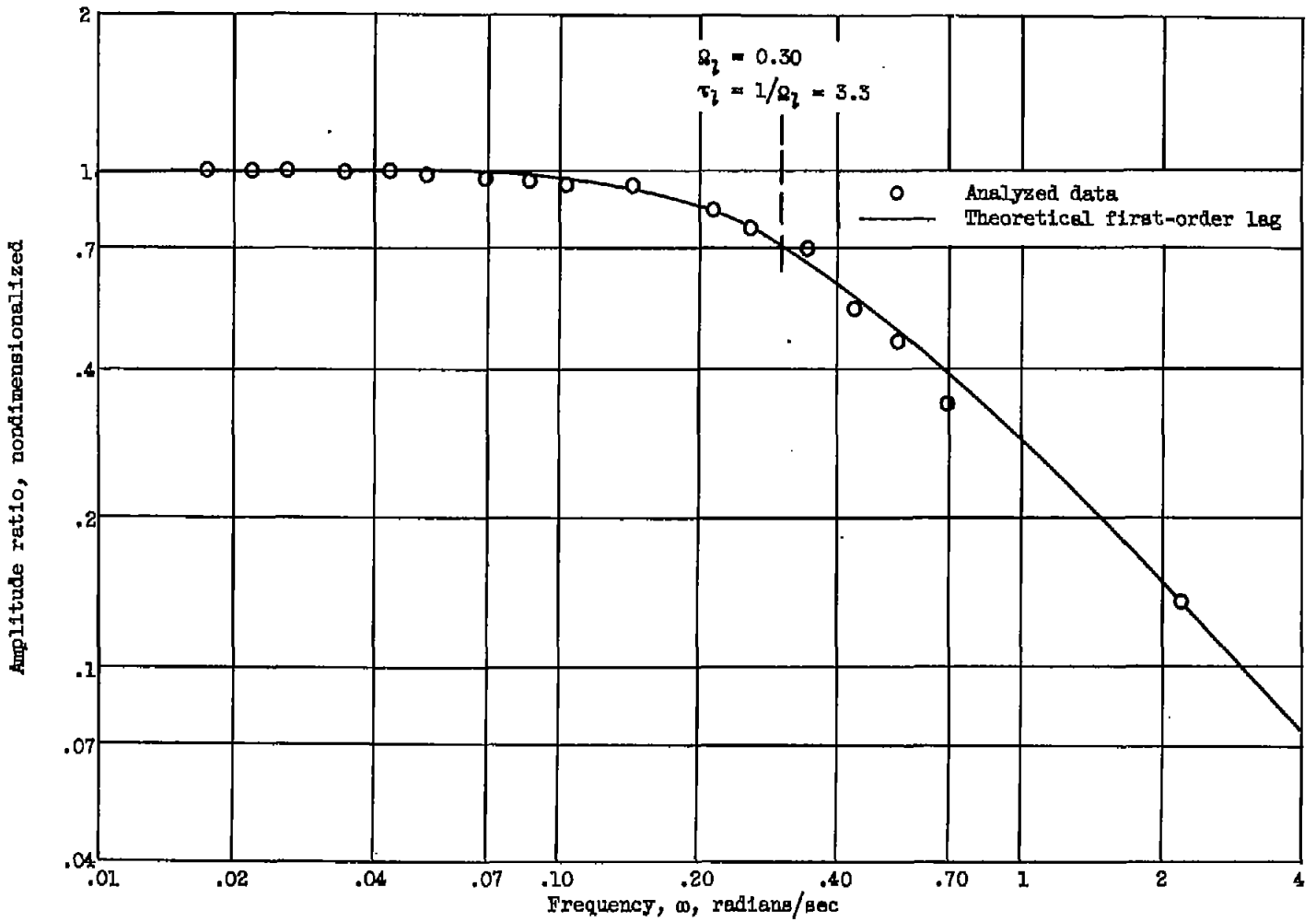

(a) Amplitude plot of ratio of leading-edge blade temperature to tail-pipe temperature.

Figure 8. - Frequency analysis of engine responses to a step in fuel flow. Altitude, 7000 feet; Mach number, 0.8; percent rated engine speed, 90 to 100.

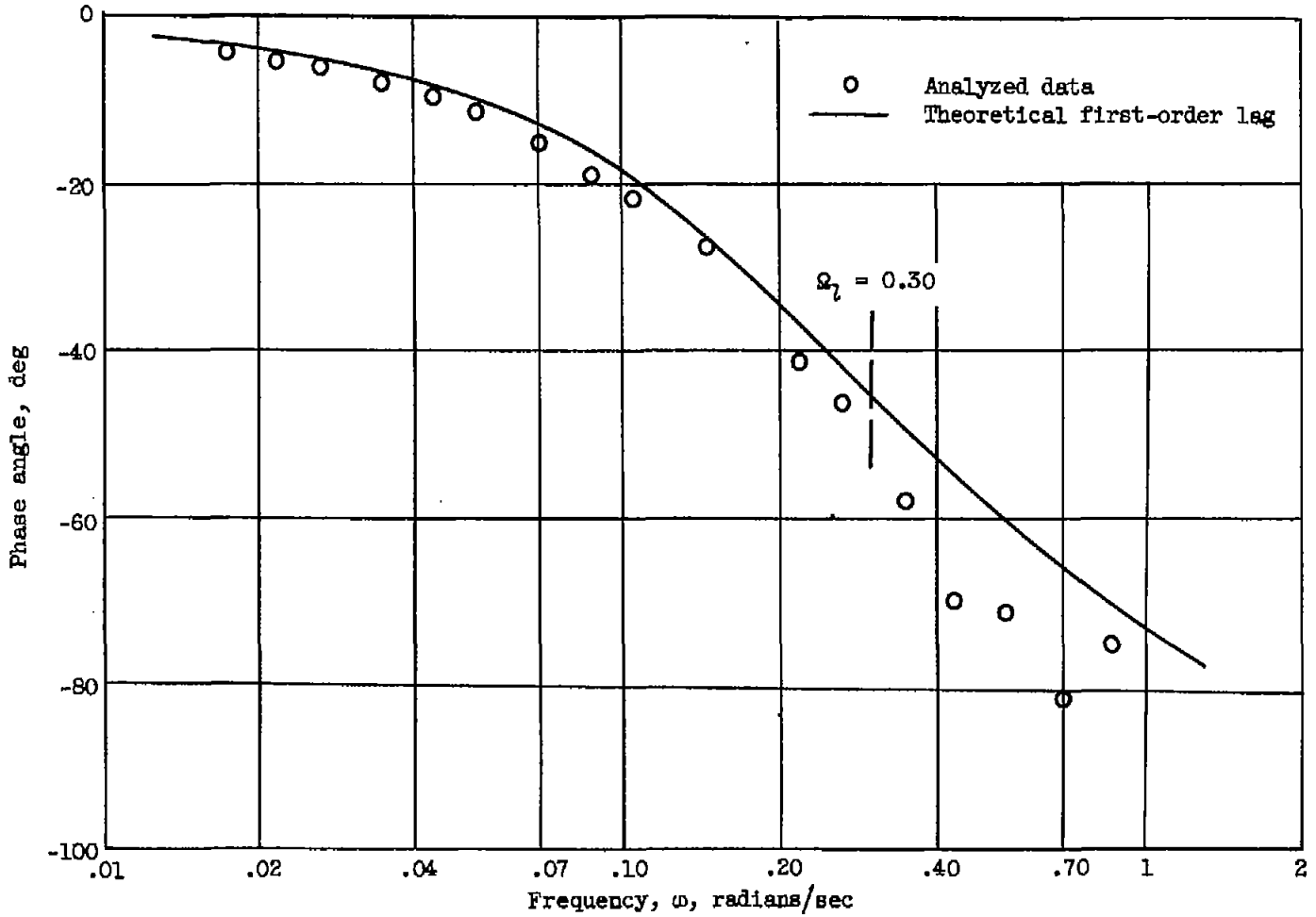

(b) Phase angle plot of ratio of leading-edge-blade temperature to tail-pipe gas temperature.

Figure 8. - Continued. Frequency analysis of engine responses to a step in fuel flow. Altitude, 7000 feet; Mach number, 0.8; percent rated engine speed, 90 to 100.

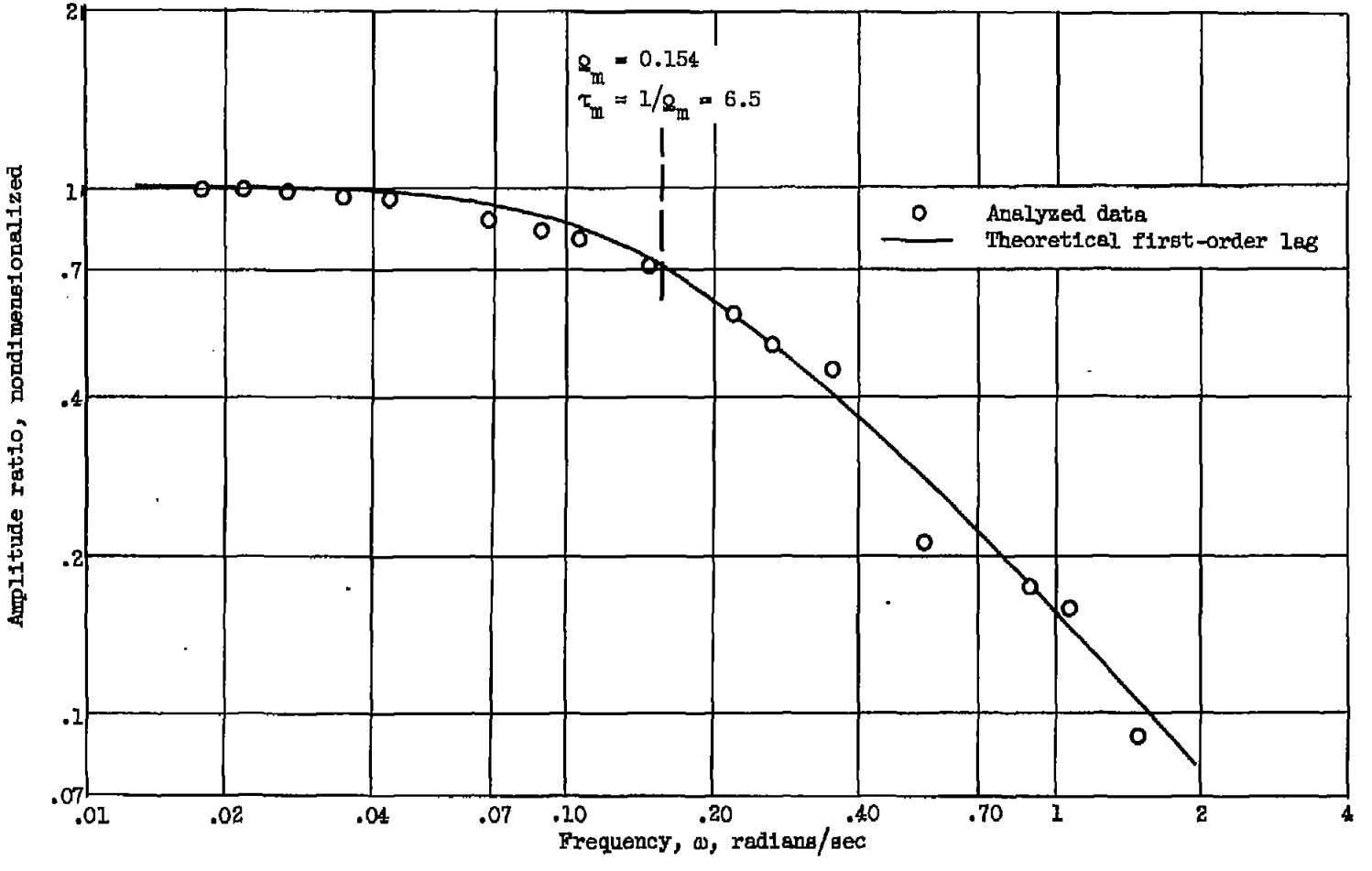

(c) Amplitude plot of ratio of midchord blade temperature to tail-pipe-gas temperature.

Figure 8. - Continued. Frequency analysis of engine responses to a step in fuel flow. Altitude, 7000 feet; Mach number, 0.8; percent rated engine speed, 90 to 100.

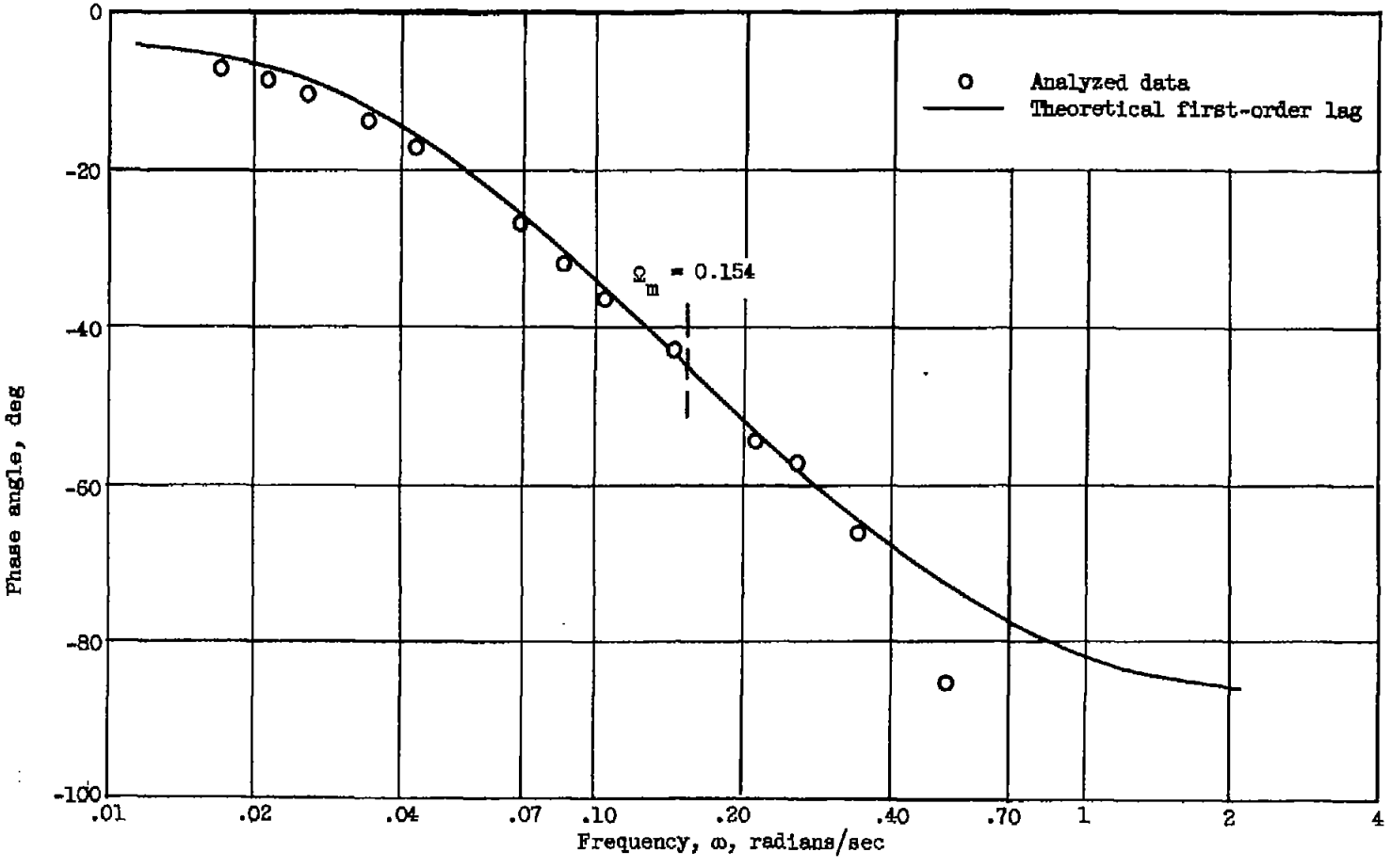

(d) Phase-angle plot of ratio of midchord blade temperature to tail-pipe gas temperature.

Figure 8. - Continued. Frequency analysis of engine responses to a step in fuel flow. Altitude, 7000 feet; Mach number, 0.8; percent rated engine speed, 90 to 100.

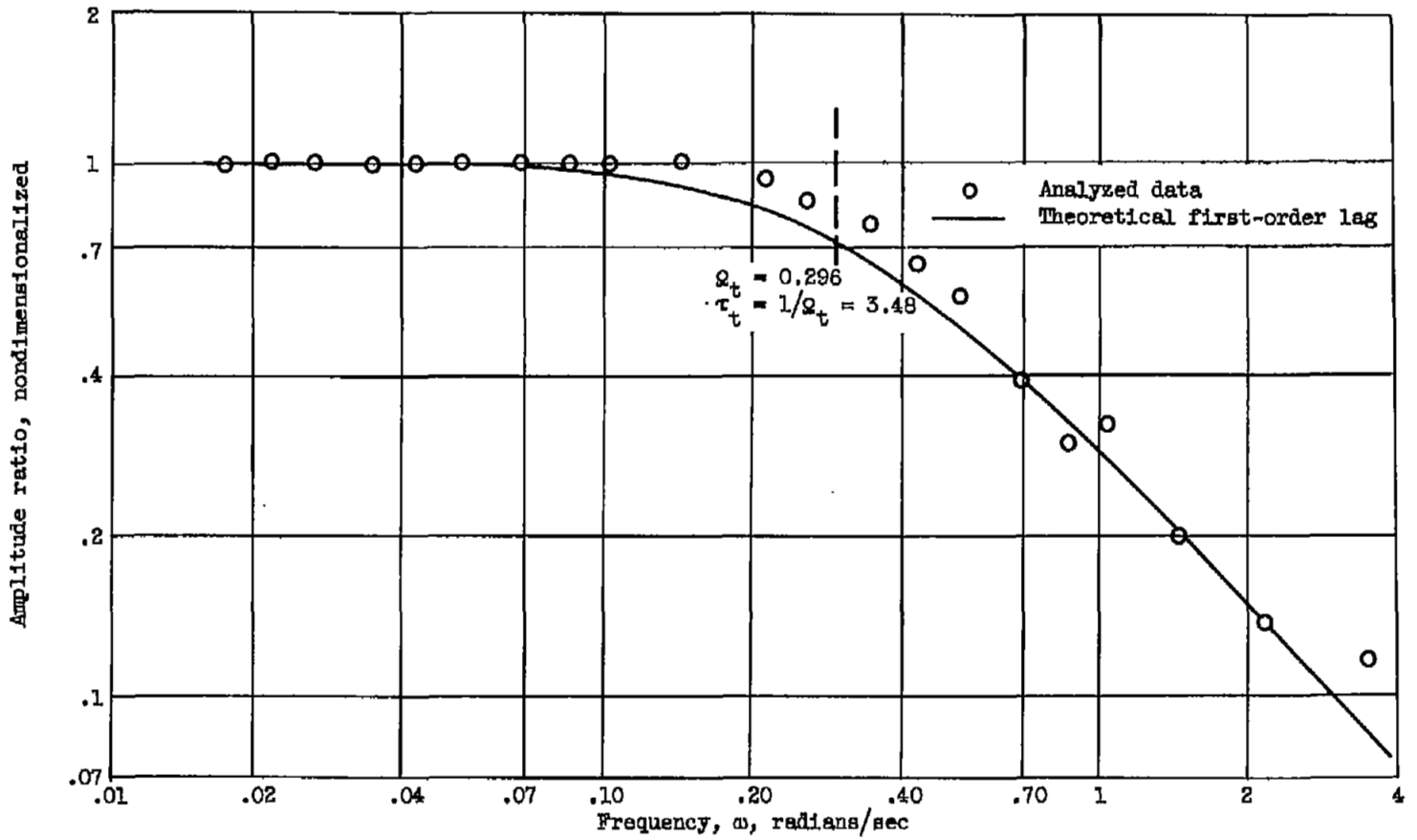

(e) Amplitude plot of ratio of trailing-edge blade temperature to tail-pipe gas temperature.

Figure 8. - Continued. Frequency analysis of engine responses to a step in fuel flow. Altitude, 7000 feet; Mach number, 0.8; percent rated engine speed, 90 to 100.

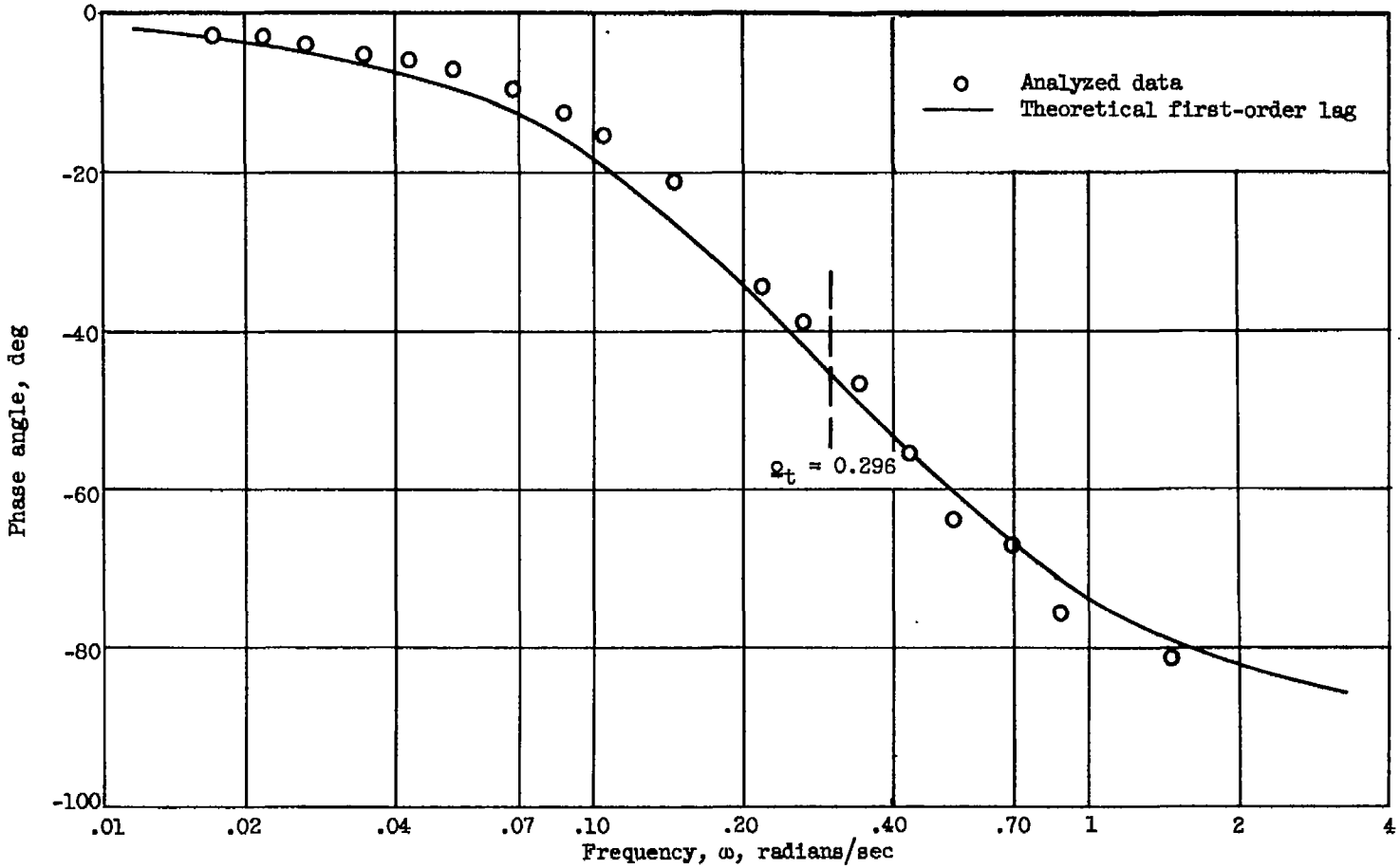

(f) Phase angle plot of ratio of trailing-edge blade temperature to tail-pipe gas temperature.

Figure 8. - Continued. Frequency analysis of engine responses to a step in fuel flow. Altitude, 7000 feet; Mach number, 0.8; percent rated engine speed, 90 to 100.

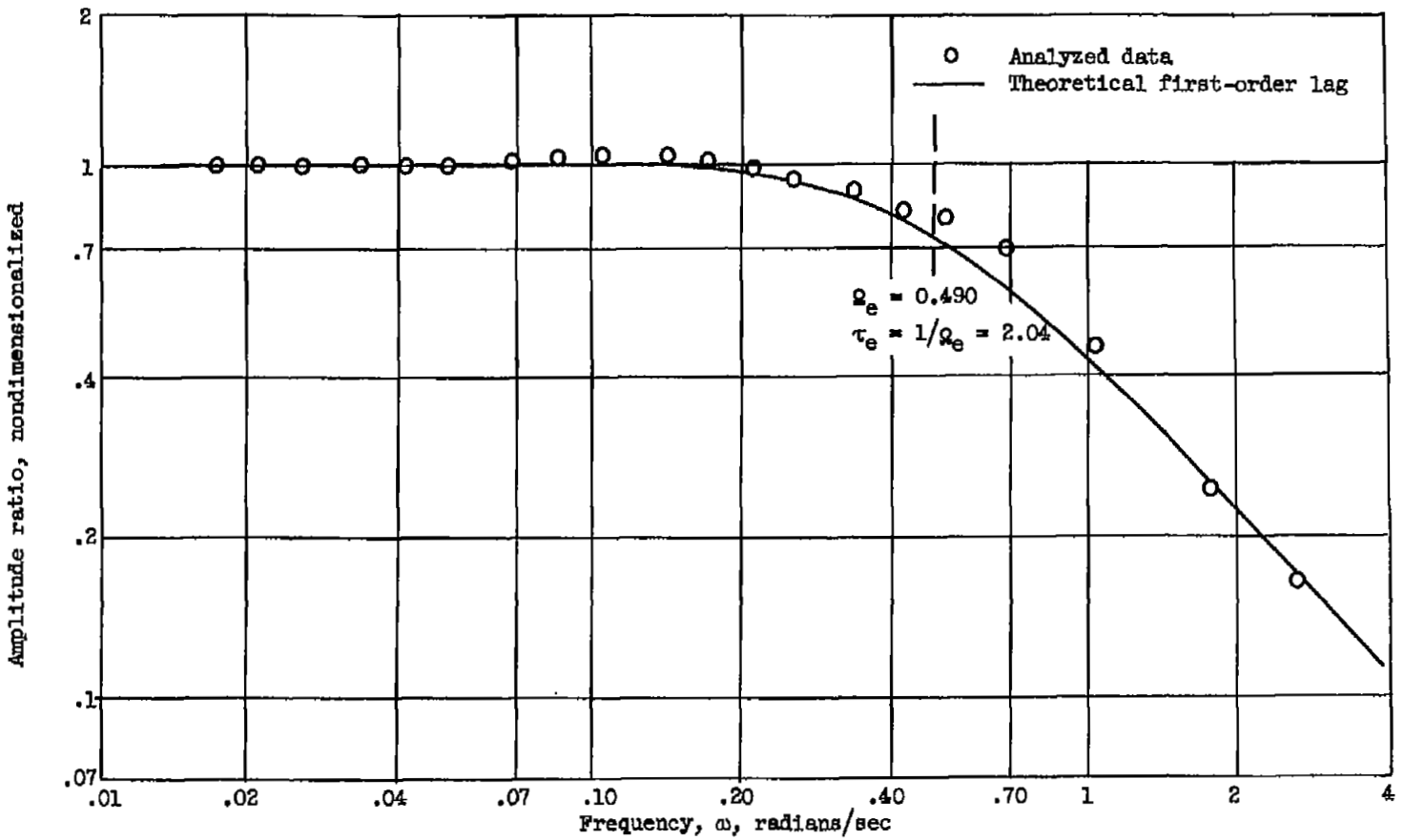

(g) Amplitude plot of ratio of engine speed to engine fuel flow.

Figure 8. - Continued. Frequency analysis of engine responses to a step in fuel flow. Altitude, 7000 feet; Mach number, 0.8; percent rated engine speed, 90 to 100.

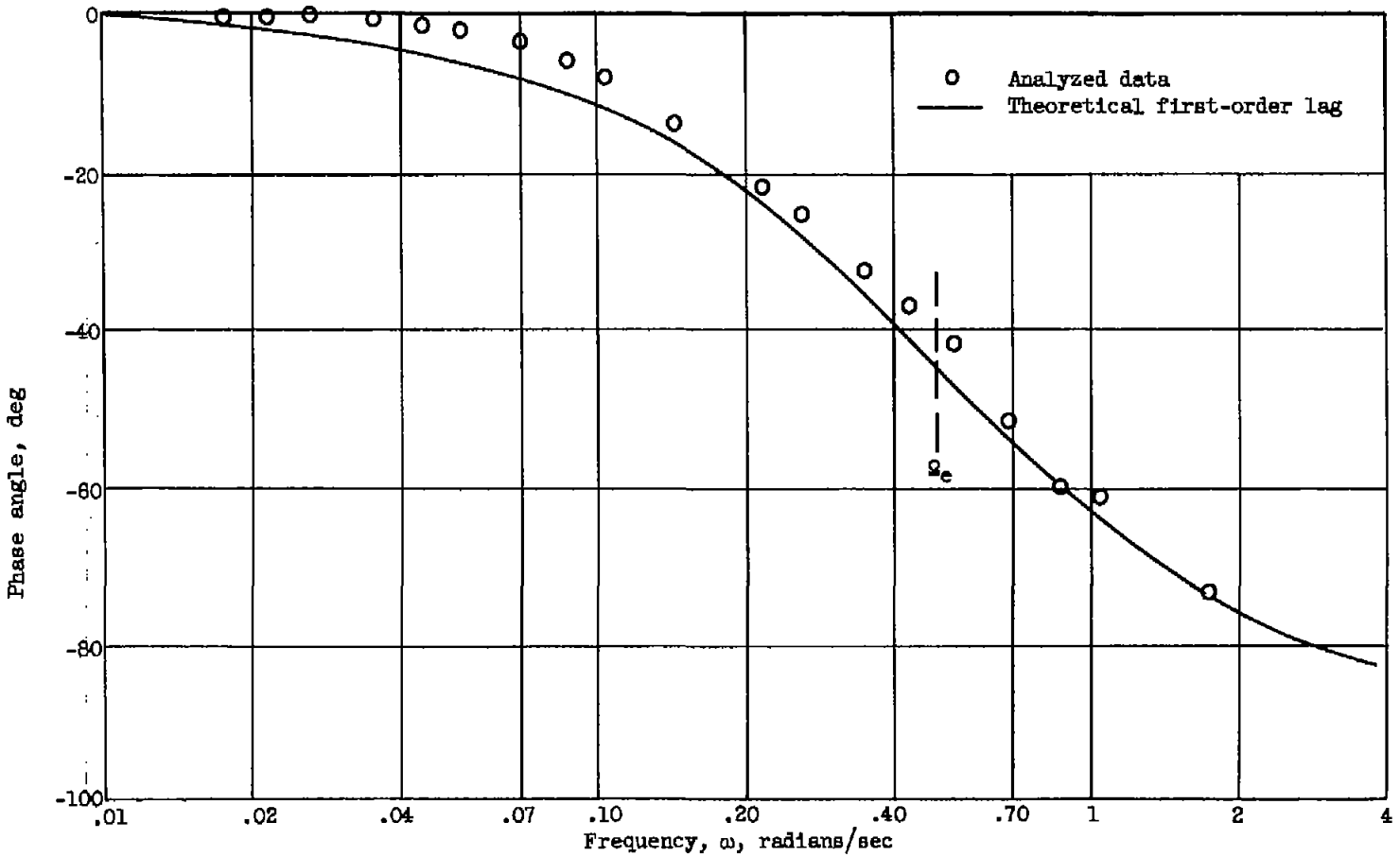

(h) Phase-angle plot of ratio of engine speed to engine fuel flow.

Figure 8. - Concluded. Frequency analysis of engine responses to a step in fuel flow. Altitude, 7000 feet; Mach number, 0.8; percent rated engine speed, 90 to 100.

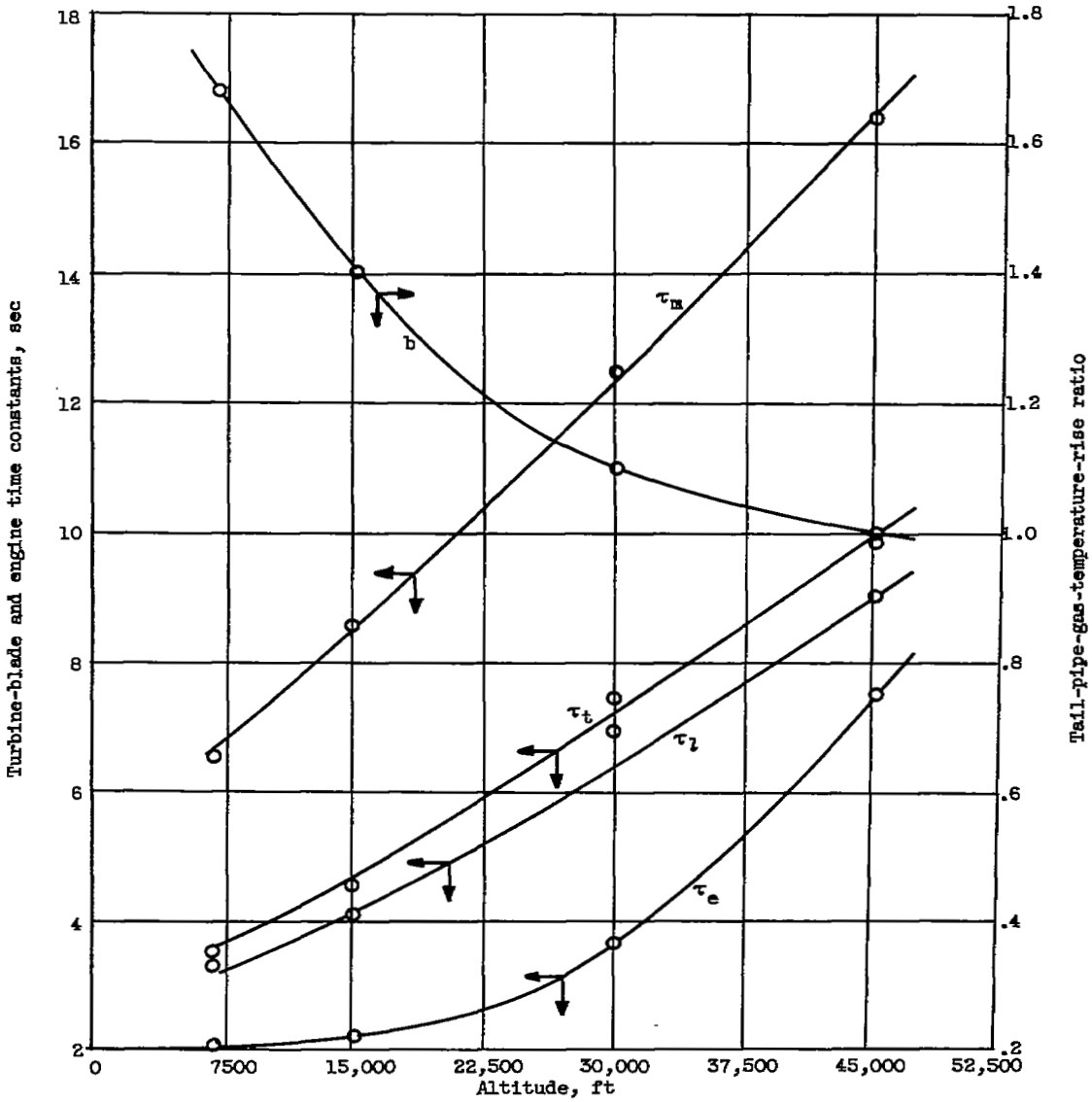

Figure 9. - Variation of transient characteristics with altitude. Mach number, 0.8; percent rated engine speed, 90 to 100.

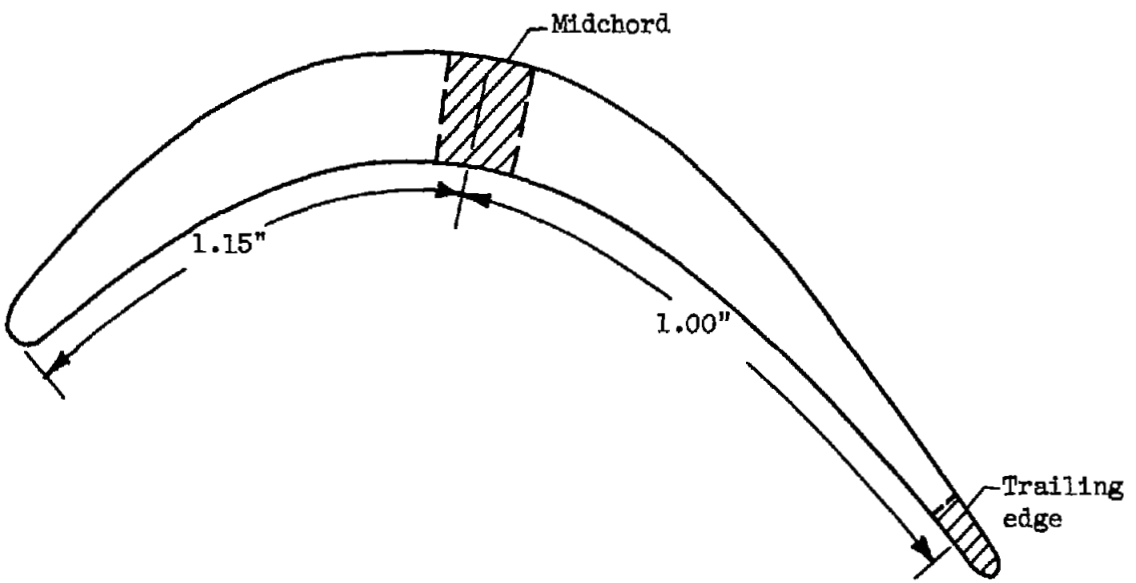

Figure 10. - Cross section of turbine blade at spanwise location considered in analysis of turbine-blade temperature dynamics. Shaded areas indicate areas considered in calculations.

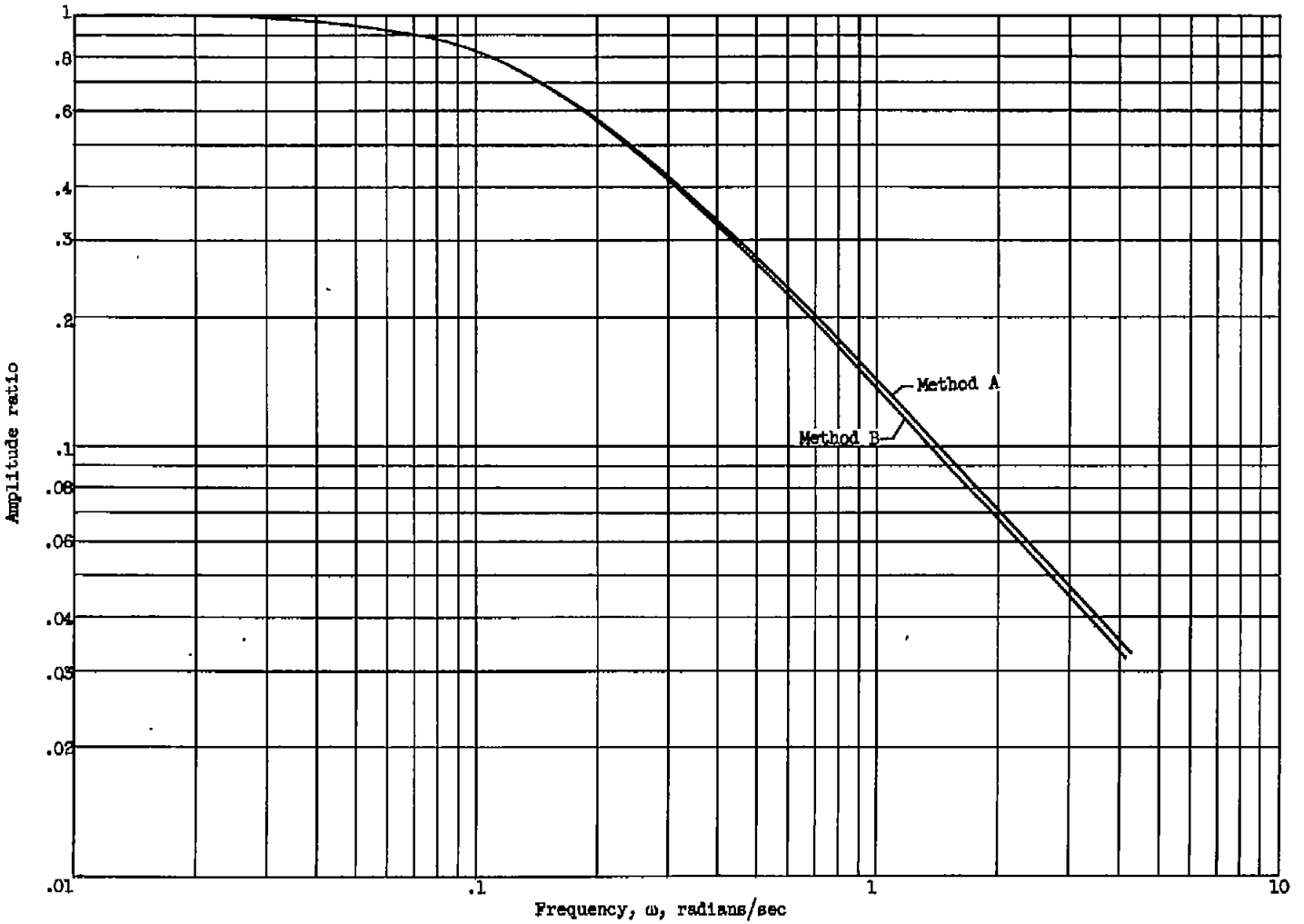

(a) Amplitude plot of ratio of midchord blade temperature to tail-pipe gas temperature.

Figure 11. - Calculated dynamic responses of turbine-blade temperatures. Altitude, 7000 feet; Mach number, 0.8; rated engine speed.

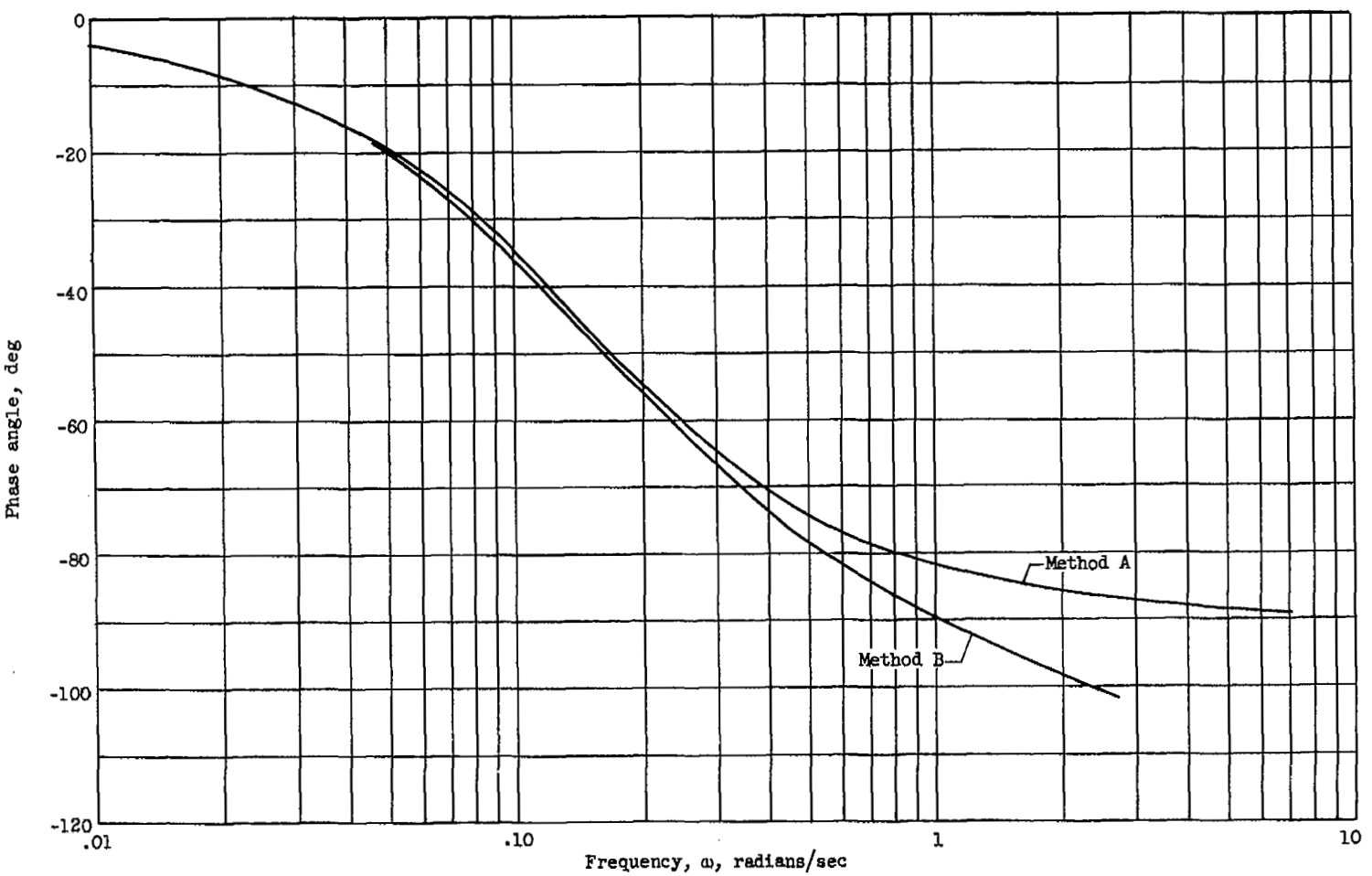

(b) Phase plot of ratio of midchord blade temperature to tail-pipe gas temperature.

Figure 11. - Continued. Calculated dynamic responses of turbine-blade temperatures. Altitude, 7000 feet; Mach number, 0.8; rated engine speed.

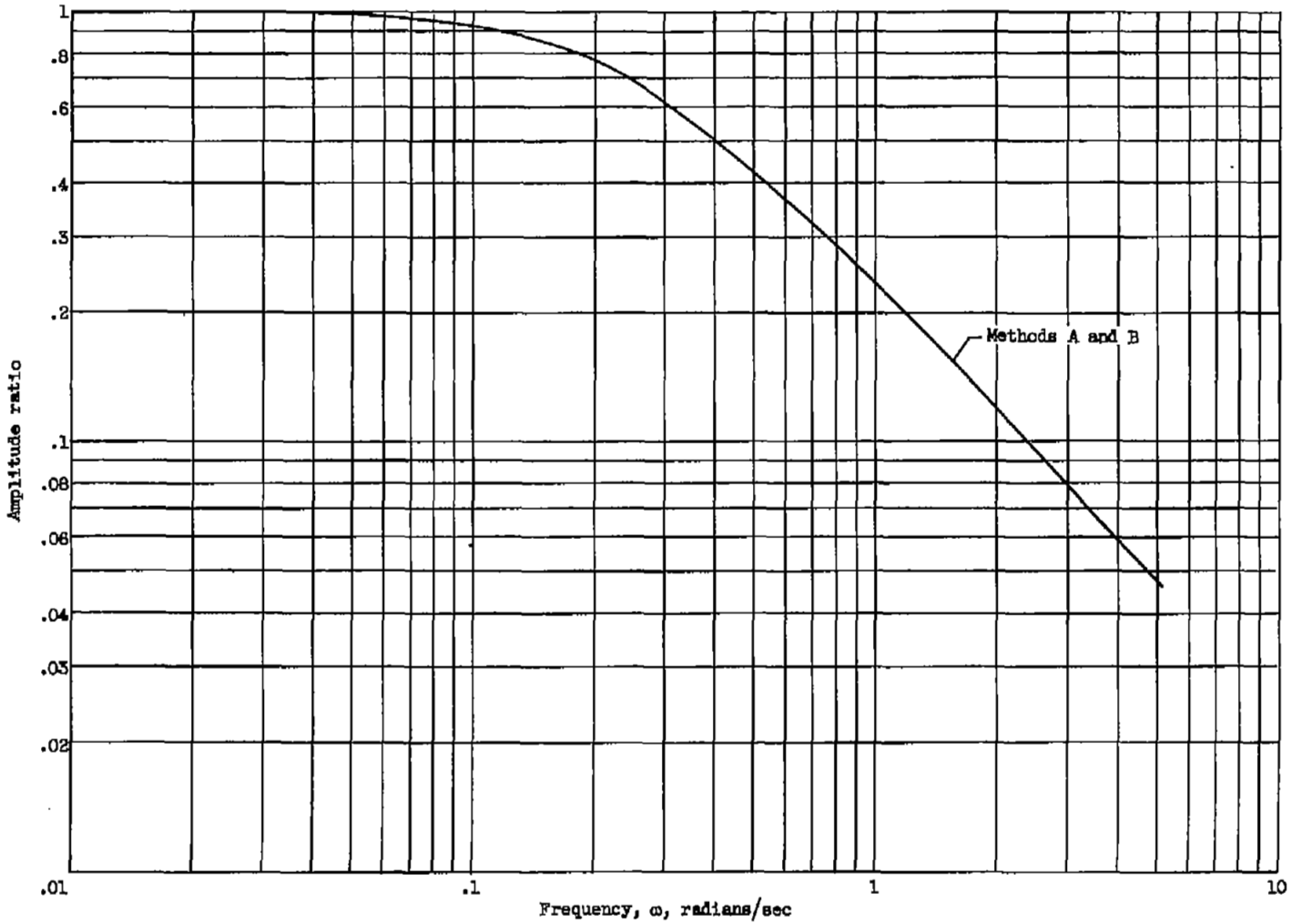

(c) Amplitude plot of ratio of trailing-edge blade temperature to tail-pipe gas temperature.

Figure 11. - Continued. Calculated dynamic responses of turbine-blade temperatures. Altitude, 7000 feet; Mach number, 0.8; rated engine speed.

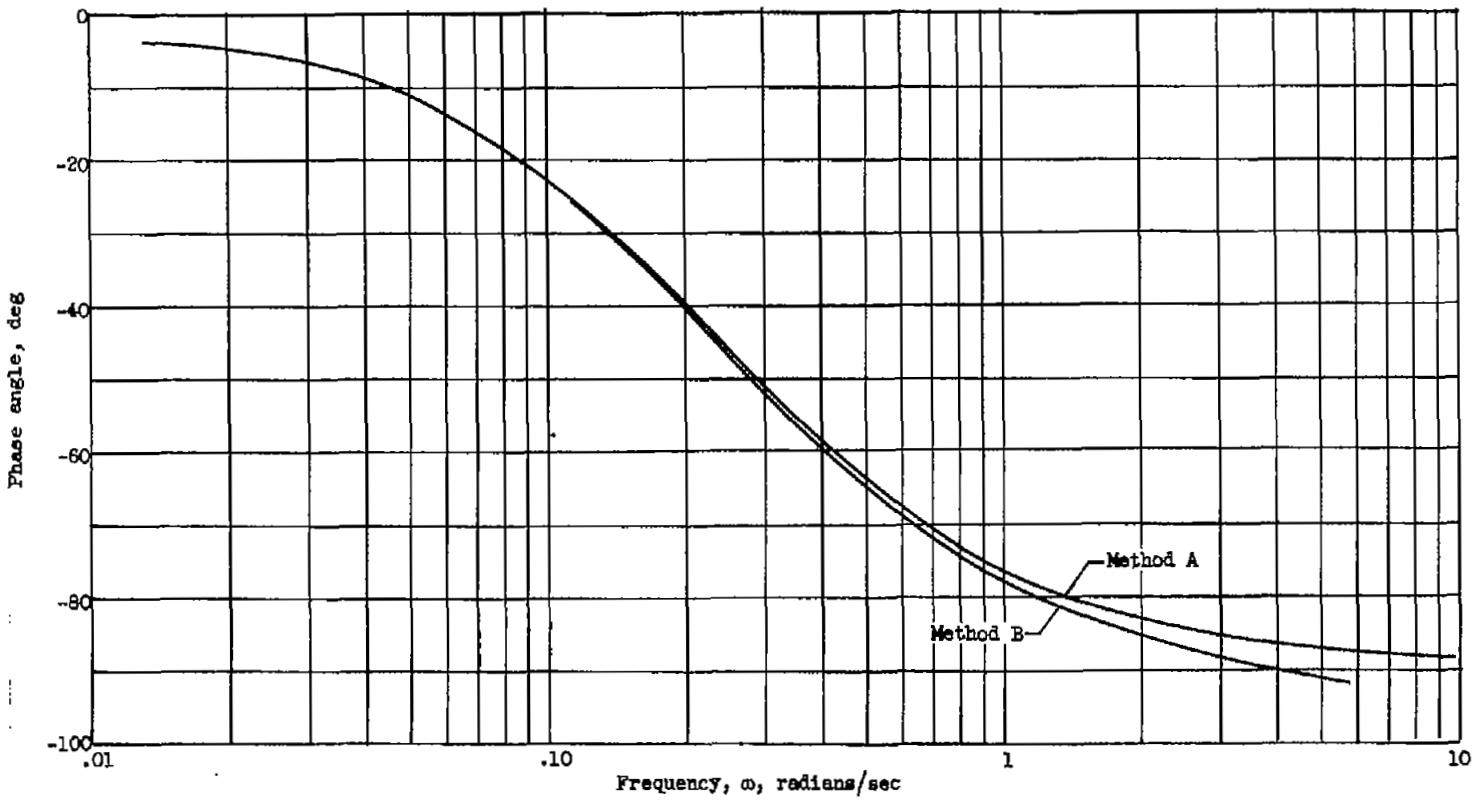

(d) Phase plot of ratio of trailing-edge blade temperature to tail-pipe gas temperature.

Figure 11. - Concluded. Calculated dynamic responses of turbine-blade temperatures. Altitude, 7000 feet; Mach number, 0.8; rated engine speed.

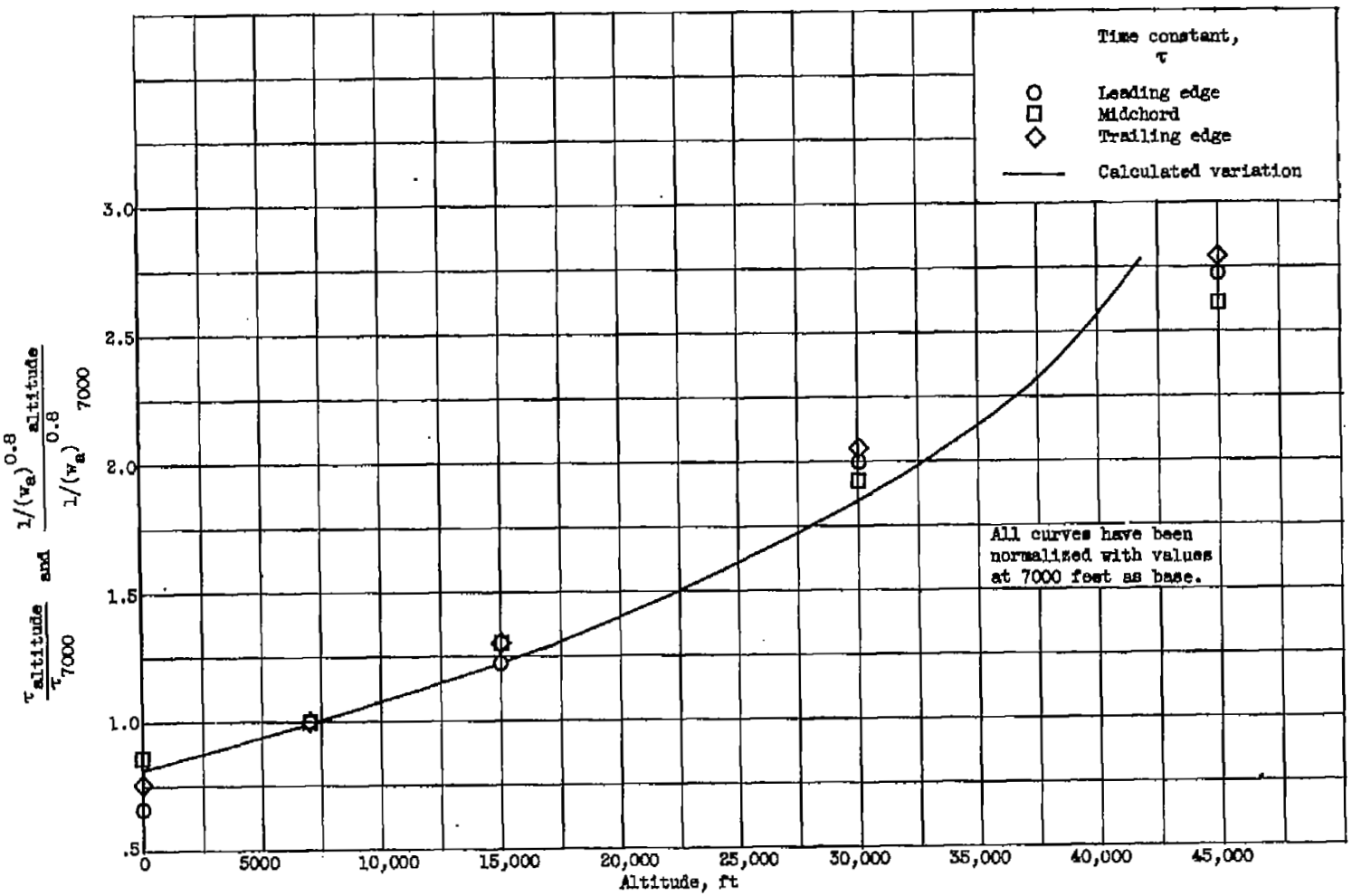

Figure 12. - Correlation of experimental turbine-blade time constants with calculated variation at varying altitude. Mach number, 0.8; rated engine speed.

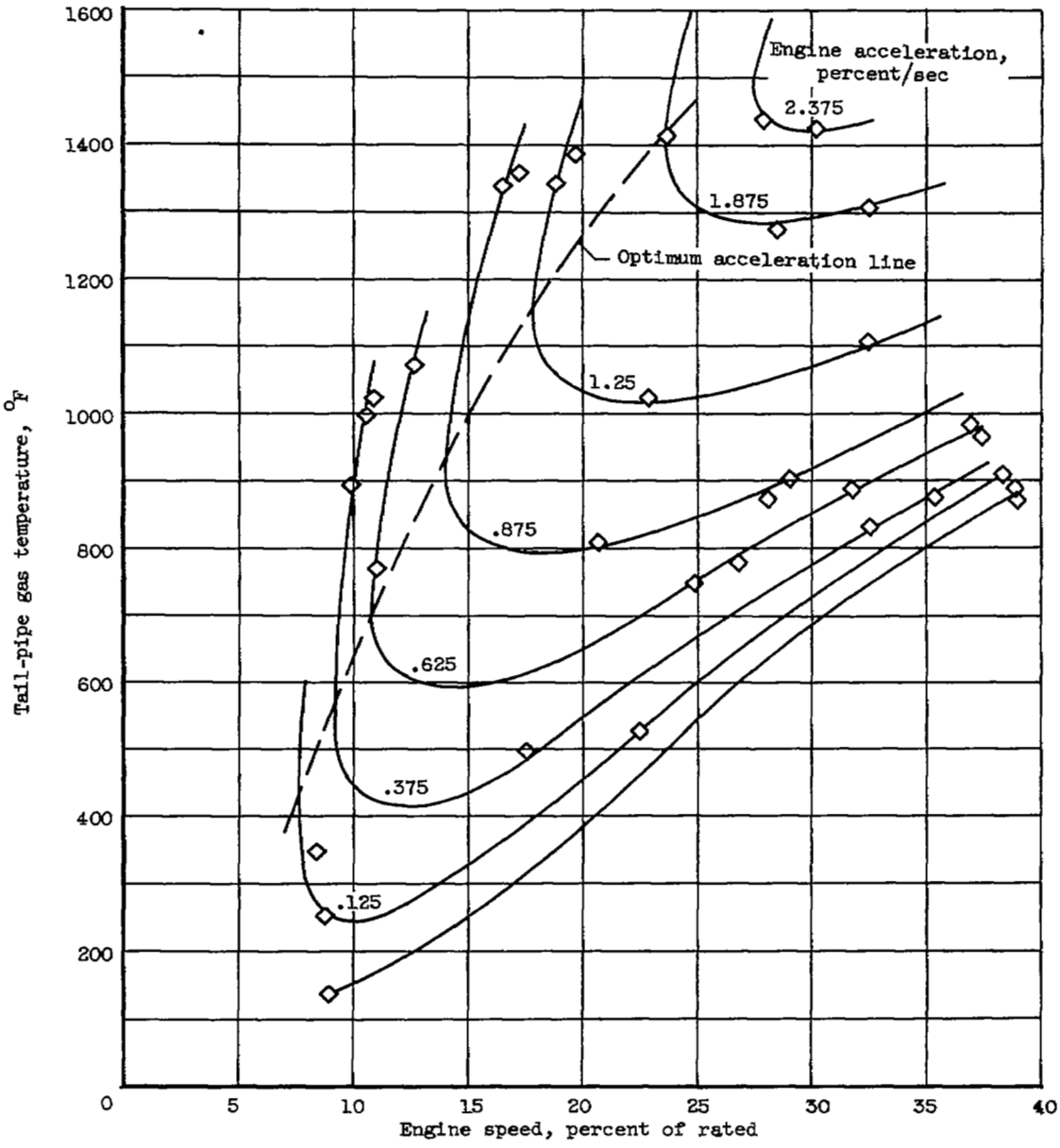

Figure 13. - Starting map of engine. Altitude, sea level; zero Mach number.

[redacted]

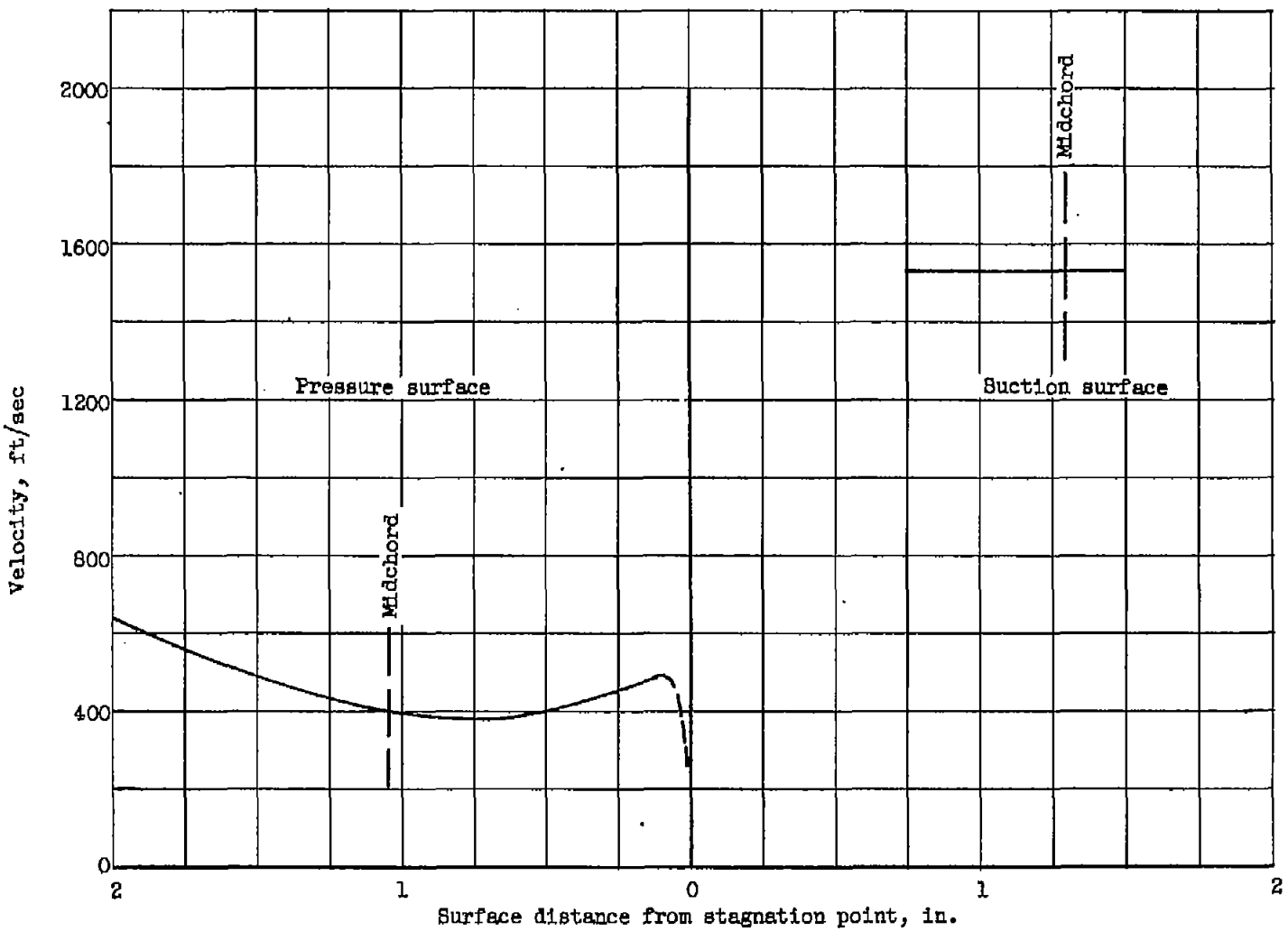

Figure 14. - Calculated turbine-blade velocity distribution.